

Bachelor's Thesis



**Czech
Technical
University
in Prague**

F3

**Faculty of Electrical Engineering
Department of Radioelectronics**

Audio Signal Processing for Optical Transmission

Jiří Nývlt

**Supervisor: Ing. Petr Honzík, Ph.D.
Field of study: Electronics and Communications
May 2023**

I. Personal and study details

Student's name: **Nývlt Jiří** Personal ID number: **499117**
Faculty / Institute: **Faculty of Electrical Engineering**
Department / Institute: **Department of Radioelectronics**
Study program: **Electronics and Communications**

II. Bachelor's thesis details

Bachelor's thesis title in English:

Audio Signal Processing for Optical Transmission

Bachelor's thesis title in Czech:

Zpracování audio signálu pro optický přenos

Guidelines:

Get familiar with digital audio signal transmission formats. Discuss the suitability of these formats for optical digital signal transmission in terms of bit rate or other parameters. Design the audio signal processing modules at the input and output of a device for optical digital signal transmission. The input module should include analogue signal pre-processing and AD conversion, the output module should include DA conversion and eventually analogue post-processing. Measure the transmission characteristics of the proposed modules.

Bibliography / sources:

- [1] VEDRAL, Josef and Jakub SVATOŠ. Analog Signal Processing and Digitalization in Measurement. Praha: VUT, 2020. ISBN 978-80-01-06717-8
[2] HAASZ, Vladimír et al. Elektrická měření: Přístroje a metody. 3. vydání. Praha: VUT, 2018. ISBN 978-80-01-06412-2

Name and workplace of bachelor's thesis supervisor:

Ing. Petr Honzík, Ph.D. Department of Radioelectronics FEE

Name and workplace of second bachelor's thesis supervisor or consultant:

Date of bachelor's thesis assignment: **13.02.2023** Deadline for bachelor thesis submission: **26.05.2023**

Assignment valid until: **22.09.2024**

Ing. Petr Honzík, Ph.D.
Supervisor's signature

doc. Ing. Stanislav Vitek, Ph.D.
Head of department's signature

prof. Mgr. Petr Páta, Ph.D.
Dean's signature

III. Assignment receipt

The student acknowledges that the bachelor's thesis is an individual work. The student must produce his thesis without the assistance of others, with the exception of provided consultations. Within the bachelor's thesis, the author must state the names of consultants and include a list of references.

Date of assignment receipt

Student's signature

Acknowledgements

I would like to thank the company METEL Ltd and its associates for allowing me to work on this project under their direction and for accommodating me in so many ways. I would also like to thank my friend and classmate Jan Šlehofer for valuable councils in the design process and throughout our entire studies. My thanks also go to Ing. Petr Honzík, Ph.D for being my supervisor and for his advice.

Declaration

I hereby declare that the presented thesis is my own work and that I have cited all sources of information in accordance with the Guideline for adhering to ethical principles when elaborating an academic final thesis.

In Prague, May 22, 2023

Prohlašuji, že jsem předloženou práci vypracoval samostatně a že jsem uvedl veškeré použité informační zdroje v souladu s Metodickým pokynem o dodržování etických principů při přípravě vysokoškolských závěrečných prací.

V Praze, 22. května 2023

Signature / Podpis:

Abstract

This thesis's main concept is the design, implementation and testing of hardware for analog processing and digitization of an audio signal for subsequent transmission over an optical line. First the basic principles of analog signal processing, digitization and optical communication are explained in the Theoretical Part, then the entire design process up to the prototype's testing is covered in the Practical Part. The contractor of this task is a company called *METEL Ltd*, which is to use this system to expand their product line of digital optical converters. The work's outcome are two devices – a transmitter and a receiver, the two of which connect with an optical fiber and which feature stereo and balanced audio inputs/outputs. Frequency response, noise and distortion measurements were performed and possible design improvements for future versions listed.

Keywords: audio, signal, A/D converter, optical transmission, analog processing, digitization, I²S

Supervisor: Ing. Petr Honzík, Ph.D.
Czech Technical University in Prague,
Technická 1902/2,
166 27 Praha 6

Abstrakt

Práce se zabývá návrhem, realizací a testováním hardwaru pro analogové zpracování a digitalizaci audio signálu pro následný optický přenos. Nejprve jsou v teoretické části vysvětleny základní principy analogového zpracování signálů, digitalizace a optické komunikace, následně je popsán celý proces návrhu prototypu a jeho testování v části praktické. Zadavatelem je firma *METEL s.r.o.*, která má zařízením rozšířit svou nabídku digitálních optických převodníků. Výstupem práce jsou dvě zařízení – vysílač a přijímač, které se propojují optickým vláknem a které disponují stereo a symetrickými audio vstupy/výstupy. Na systému byly provedeny měření frekvenčních charakteristik, šumu a zkreslení. Výsledky měření byly zhodnoceny včetně potenciálních vylepšení v návrhu pro budoucí verze.

Klíčová slova: audio, signál, A/D převodník, optický přenos, analogové zpracování, digitalizace, I²S

Překlad názvu: Zpracování audio signálu pro optický přenos

Contents

Introduction	1	4.1.8 Power Supply Circuits	37
Part I		5 Design	39
Theoretical Part		5.1 Transmitter	39
1 Analog Processing of Audio Signals	7	5.1.1 Preamplifier	39
1.1 Noise	8	5.1.2 A/D Converter	41
1.1.1 Thermal Noise	9	5.2 Receiver	43
1.1.2 Shot Noise	9	5.2.1 D/A Converter	43
1.1.3 Flicker Noise	9	5.2.2 Audio Balancer	45
1.2 Distortion	10	5.2.3 Audio Detector	47
1.3 Operational Amplifiers	11	5.3 Switching Circuits	49
1.4 Microphones	13	5.4 Power Supply	50
1.4.1 Condenser	13	5.5 Clock	52
1.4.2 Electret	14	5.6 PCB design	53
1.4.3 Dynamic	15	6 Testing	55
2 Digitization of Audio Signals	17	6.1 Line Audio	56
2.1 Sampling	17	6.1.1 Frequency Response	56
2.2 Quantization	19	6.1.2 THD+N	61
2.3 Coding	21	6.1.3 SNR	63
2.4 Delta-Sigma Converters	21	6.1.4 Summary	63
2.4.1 Delta-Sigma Modulation	21	6.2 Microphone Preamplifier	64
2.4.2 Delta-Sigma A/D Converters	22	6.2.1 Frequency Response	65
2.4.3 Delta-Sigma D/A Converters	23	6.2.2 THD+N	66
2.4.4 Digital Filters	23	6.2.3 SNR	66
2.5 Serial Protocols for Digital Audio		6.2.4 CMRR	67
Transmission	25	6.2.5 Summary	68
2.5.1 I ² S	25	6.3 Audio Balancer	71
2.5.2 TDM	25	6.3.1 Frequency Response	71
2.5.3 PDM	26	6.3.2 THD+N	71
3 Optical Communication	27	6.3.3 SNR	74
3.1 Optical Transmitter	28	6.3.4 Summary	75
3.2 Optical Fiber	28	6.4 Miscellaneous	76
3.3 Optical Receiver	29	Conclusion	77
Part II		Bibliography	79
Practical Part		Appendices	
4 Specifications	33	A List of Abbreviations	85
4.1 Component Selection	34		
4.1.1 Capacitors	35		
4.1.2 A/D Converter	35		
4.1.3 D/A Converter	35		
4.1.4 Operational Amplifiers	36		
4.1.5 I/O Connectors	36		
4.1.6 Switches	37		
4.1.7 Clock	37		

Figures

<p>1 Equivalent circuit model of a metallic transmission line as described in [3] 2</p> <p>1.1 ADA4622-2 voltage noise spectral density from [9] 10</p> <p>1.2 Equivalent circuit of an operational amplifier with static error parameters from [13], p. 6 (XII-6/39) 11</p> <p>1.3 Impact of finite slew rate on Op Amp's output signal u_{o2r} from [13], p. 25 (XII-25/39) 12</p> <p>1.4 Simplified principle diagram of a capacitor microphone function based on the contents of [14] 14</p> <p>2.1 Sampling in the time domain 18</p> <p>2.2 Sampling in the spectral domain for $f_s/2 > f_m$ 18</p> <p>2.3 Sampling in the spectral domain for $f_s/2 < f_m$ 19</p> <p>2.4 Quantization in the time domain 19</p> <p>2.5 Quantization noise spectral distribution for $f_{s4} = 2f_{s2} = 4f_s$ 20</p> <p>2.6 Delta sigma modulator simplified schematic from [18], p. 425 22</p> <p>2.7 The delta-sigma ADC block diagram based on the contents of [19] 22</p> <p>2.8 The delta-sigma DAC block diagram based on the contents of [20] 23</p> <p>2.9 I²S signal waveforms based on the contents of [16] 25</p> <p>2.10 TDM signal waveforms based on the contents of [16] 26</p> <p>3.1 A principle diagram of an optical transmission path based on the contents of [23] 27</p> <p>3.2 Ray refraction and ray reflection in an optical fiber based on the contents of [23] 29</p> <p>4.1 An industrial PLC from the contractor's IPLOG-GAMA series using the same aluminium chasis as the intended product 34</p>	<p>4.2 NCJ6FA-H: 3 pole XLR female receptacle with 6.3 mm stereo jack, horizontal PCB mount from [28] 36</p> <p>4.3 D4006RP dip switch from OMEGA FUSIBILI commonly used by the contractor 37</p> <p>5.1 The transmitter's principle block diagram 39</p> <p>5.2 Full schematic of the preamplifier 40</p> <p>5.3 Simulated differential amplifier output (with removed DC component from Op Amp bias) for 1 kHz sinusoidal input with added common noise from LTSpice 40</p> <p>5.4 Simulated preamplifier's frequency response for a 38 dB gain from LTSpice 41</p> <p>5.5 Input XLR connection to preamplifier 41</p> <p>5.6 A/D converter full schematic 42</p> <p>5.7 Pin function description for pins MD6, MD5 and MD2 from PCM1861 datasheet [25] 43</p> <p>5.8 The receiver's principle block diagram 43</p> <p>5.9 Full D/A converter schematic 44</p> <p>5.10 Audio balancer schematic 45</p> <p>5.11 Simulated balancer's output signals for a 1kHz sine wave input from LTSpice 46</p> <p>5.12 Balancer's AC analysis from LTSpice 46</p> <p>5.13 Audio detector schematic - 1st version 47</p> <p>5.14 Audio detector schematic - 2nd version 48</p> <p>5.15 Dip switch and jumper schematic 49</p> <p>5.16 TS3A24157 switches schematic 50</p> <p>5.17 Phantom power switching schematic 50</p> <p>5.18 Input power supply circuit schematic 51</p> <p>5.19 Analog 3.3 V power supply schematic with LT3012B 51</p> <p>5.20 The clock distribution circuit schematic 52</p>
--	--

5.21 The designed unmounted PCB	53	6.16 FFT of the preamp's output's noise for a gain of 20 dB	67
6.1 R&S UPV audio analyzer from the manufacturer's website [32]	55	6.17 Measured CMRR of the differential stage in relation to frequency	68
6.2 The system's measured line audio magnitude response from 20 Hz to 20 kHz with and IIR decimation and interpolation filter	56	6.18 A <i>Superbal</i> input amplifier from [4], p. 509	69
6.3 The system's measured line audio magnitude response from 20 Hz to 20 kHz with an FIR decimation and interpolation filter	57	6.19 Simple hybrid microphone preamplifier from [4] p. 501	70
6.4 The system's measured line audio magnitude response from 20 Hz to 80 kHz	58	6.20 The balancer's measured frequency response	71
6.5 The system's measured phase response for an IIR and FIR interpolation and decimation filter	58	6.21 FFT of the balancer's output measured for a 0.5 V _{RMS} sine wave 1 kHz input	72
6.6 The system's unwrapped phase response for an IIR and FIR interpolation and decimation filter	59	6.22 FFT of the balancer's output measured for a 1 V _{RMS} sine wave 1 kHz input	73
6.7 The system's group delay response for an IIR and FIR interpolation and decimation filter	59	6.23 TL972 dependence of THD+N on the output's RMS voltage for a 2.7 V power supply voltage from the part's datasheet [27]	73
6.8 The system's group delay response for an IIR interpolation and decimation filter in detail	60	6.24 TL972 dependence of THD+N on the output's RMS voltage for a 5 V power supply voltage from the part's datasheet [27]	74
6.9 The system's group delay response for na FIR interpolation and decimation filter in detail	60		
6.10 Left channel output's spectrum measured for a 1 kHz sine wave input	61		
6.11 Right channel output's spectrum measured for a 1 kHz sine wave input	62		
6.12 Original differential amplifier schematic	64		
6.13 Updated differential amplifier schematic	64		
6.14 The preamplifier's measured frequency response for a gain of 16 dB	65		
6.15 The preamplifier's measured frequency response for a gain of 40 dB	65		

Tables

5.1 Series resistors on clock lines mounting variants	52
6.1 Line audio's measured THD+N values	61
6.2 Harmonics amplitudes in the output's spectrum for both line audio channels	62
6.3 Line audio's SNR for different filters	63
6.4 The preamplifier's THD+N and THD values for different gains	66
6.5 Preamplifier's SNR values for different gains and two different filters	66
6.6 Balancer's THD+N values for different input levels	72
6.7 Balancer's SNR values for different input levels and two different filters	74
6.8 The balancer's noise RMS values	75



Introduction

Although metallic transmission lines still dominate in communication and network industry, as they have for over a hundred years due to their affordability and reliability, optical fiber connections are becoming more and more popular due to their many advantages when compared to a standard copper wire. These include, among others, higher bandwidth, lower attenuation and a complete electromagnetic interference (EMI) immunity. They also allow for wavelength multiplexing which further enhances their information capacity. The only virtual disadvantage of an optical fiber is its higher production and installation cost. The article [1] discusses this topic and served as one of the main sources of information for the entire Introduction of this thesis.

The above-mentioned characteristics of an optical fiber is what makes them an appropriate choice for long distance backbone connections, which is where they are very likely to be found in the case of most major companies. However, with the optical fiber production cost decreasing over time they have become suitable even for lower level interconnections and are now a standard feature in many consumer electronic devices. The current main limitations of optical systems is the signal conversion from optical to electrical and vice versa, which is often necessary multiple times along the transmission path [2].

Transmitting high quality audio signal over a metallic transmission line can become complicated with increasing distances. As described in [3], the equivalent circuit model of a metallic transmission line can be represented by two series terms of resistance and inductance and two shunt terms of capacitance and conductance as it is to be seen in Figure 1.

Figure 1 shows, that the longer the transmission line is, the higher the series impedance and the lower the shunt impedance gets, which leads to high frequency cut-off as well as to an overall attenuation of an audio signal. Another pitfall of metallic wires is the susceptibility to electromagnetic interference from either other data transmission lines, power lines or RF sources, which also arises with increasing cable length.

To reduce the effects of EMI the so-called *balanced* audio is often used, which as described in [4] is transmitted over a three-wire connection with two anti-phase audio signals and one common ground. The resulting signal is obtained by subtracting the two audio signals thereby eliminating any

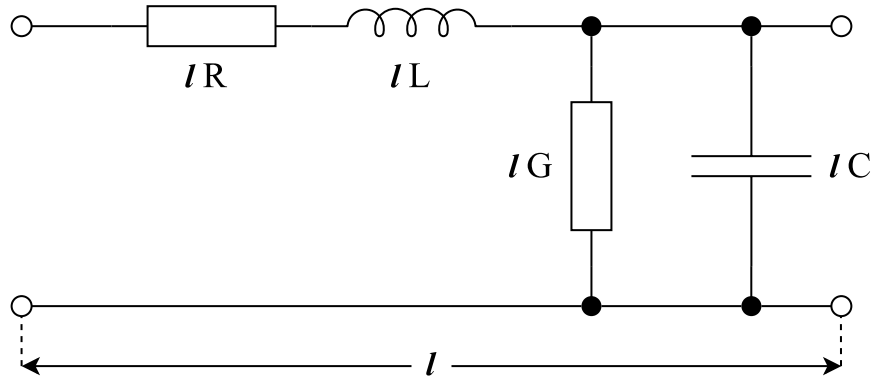


Figure 1: Equivalent circuit model of a metallic transmission line as described in [3]


interference that was induced on them along the transmission path. Such a method though it is resistant to EMI, it is still subject to the wire's attenuation caused by its parasitic impedance, and therefore becomes insufficient with increasing lengths.

While transmitting audio in a digital form is also highly immune to interference, the transmission line's parasitic impedances in this case limit the available bandwidth and therefore don't allow for higher data rates.

Transmitting audio over an optical fiber solves all these issues, as optical fiber has according to [1] a complete immunity to electromagnetic interference, has a much lower attenuation which allows for longer distance transmission while also having a virtually flat frequency dependence of attenuation up until very high frequencies, which allows for much higher data rates and therefore a higher possible resolution of digital audio. Furthermore, an optical fiber ought to be lighter and thinner than copper wires.

In order for an audio signal to be transmitted over an optical fiber, numerous signal processing tasks are to be performed first. Among them are mainly analog to digital conversion, subsequent serialization of the digital data and finally an electrical to optical conversion. Prior to digitization, analog processing methods such as filtering or amplifying may be desirable or even necessary. For an audio signal to be reconstructed from an optical receiver, after converting the optical signal to an electrical signal, deserialization and digital to analog conversion is to be performed and possibly some analog processing methods likewise.

This thesis aims to outline the basic principles of the above-mentioned processing tasks along with other related topics which are important to consider when designing a high quality audio transmission system. The goal is to get familiar with parameters of audio signals such as noise and distortion and their role in audio signal processing, analog signal processing along with the digitization of audio signals and its parameters, different digital signal transmission formats and their suitability for an optical conversion.



The acquired knowledge is then to be used to design and test a fully functioning prototype of an audio optical transmission system for possible future applications in e.g. theaters, concert halls, schools, cinemas, stadiums, or any live events, which require a real-time audio transmission over a long distance.



Part I

Theoretical Part

Chapter 1

Analog Processing of Audio Signals

A signal is essentially an observation of a certain physical phenomenon expressed as a function of time. As stated in [5]:

"In short, any time-varying phenomenon which conveys some information is a signal." (Puthusserypady [5], 2021, p. 29).

The main source of information for the following paragraphs is [6]. A signal in continuous time can be described by the following parameters

- Amplitude,
- Frequency spectrum,
- Phase spectrum.

By analog signal processing we usually mean alternating one or more of the above. Consider for example the following single-tone harmonic signal

$$s(t) = A_m \sin(\omega t + \phi), \quad (1.1)$$

where A_m is the amplitude, ω is the angular frequency and ϕ is the initial phase of a signal.

Considering that an audio signal is like all signals in nature initially analog (i.e. continuous in time), it is appropriate and many times inevitable to use analog methods in its processing. For analog methods of signal processing to be applied to a signal, signals must be first converted into the electrical domain. For audio signals this is typically done by a microphone, which is a transducer converting sound pressure to voltage, and is to be described in more detail in Section 1.4.

Although many processing methods are now applied in the digital domain, analog signal processing still has its place in audio electronics due to its speed, precision, lower power consumption and in many cases lower cost than a digital implementation of the same processing task. Furthermore, while digital signal processing is effectively completely noise-resistant, the digitization itself is inevitably accompanied by a *quantization error* which is a form of noise and is to be examined in more detail in Section 2.2 about quantization.

Other errors can occur during digitization such as a clock error which can lead to severe distortion of the digitized signal.

The need for analog signal processing occurs especially when digitizing an analog signal from a low-output source such as a microphone. Namely an analog front-end circuitry to amplify that signal to a workable value for the analog-to-digital (A/D) converter. As is written in [4]:

"There is clearly little prospect of ever being able to connect an A-to-D converter directly to a microphone. The same applies to other low-output transducers such as moving-coil and moving-magnet phono cartridges." (Self [4], 2015, p. xxii).

Audio signal processing is often like many other fields of analog signal processing demanding when it comes to accuracy. That brings requirements on noise and signal distortion¹, which inevitably accompany analog signal processing and play a fundamental role in evaluating the quality of an audio system. Both noise and distortion will therefore be examined in the following sections.

1.1 Noise

Noise refers to a random signal, which in case of an audio device is generated by the used electronic components. The time waveform of noise is due to its randomness impossible to predict, although its behavior when averaged over a long enough period of time can be described statistically and then somewhat predicted [7].

The term noise is often confused with unwanted signals whose sources are typically other electronic devices. These signals are, however, properly referred to as interference or EMI, their time waveforms are more easily predicted than in the case of noise and their role in audio was partially outlined in the Introduction.

Noise is, as described in [7], present in all electronic systems, where it is superimposed on the signal carrying information. Its effect on the processed signal is indicated by the parameter SNR (Signal-to-Noise Ratio), defined by the following equation

$$\text{SNR} = 10 \log \left(\frac{P_s}{P_n} \right), \quad (1.2)$$

where P_s is the signal power and P_n is the noise power as stated in [6].

Unless stated otherwise, noise is assumed to have a normal (Gaussian) amplitude distribution and theoretically constant spectral density across the entire frequency spectrum (i.e. *white noise*) [8]. Noises with different spectral contents are given a color according to their spectrum's similarity to the visible light spectrum (e.g. *pink noise*, *brown noise*) [4].

¹in this thesis distortion refers to non-linear distortion, where new frequency components are added to a signal

■ 1.1.1 Thermal Noise

Also known as *Johnson* noise, thermal noise occurs on all resistive elements in a circuit. The RMS value of thermal noise is according to [8] given by the equation

$$U_n = \sqrt{4k_BTR}, \quad (1.3)$$

where $k_B = 1.38 \times 10^{-23} \text{J/K}$ is the Boltzmann constant, T is temperature and R is the resistance.

Thermal noise has the characteristics of *white noise*, although in reality due to the parasitic parallel capacity of a resistor low pass filtering occurs [4] – such filtering will not have an effect in audio applications, as the audible frequencies are far lower than the inverse value of the time constant of a thusly created low pass filter.

■ 1.1.2 Shot Noise

It is caused by the time discontinuity of current through a semiconductor PN junction [8], as electrical current isn't truly continuous but rather a motion of charged particles, which varies in time in an unpredictable way, thus causing noise.

It can be modelled by a pulse current source, where the RMS current value is according to [7] equal to

$$I_n = \sqrt{2qBI}, \quad (1.4)$$

where $q = 1.6 \times 10^{-19} \text{C}$ is the charge of an electron, B is the bandwidth and I is the mean current value (DC component). For high-end audio applications the bandwidth will be typically the entire audible spectrum, i.e. 20 Hz to 20 kHz.

■ 1.1.3 Flicker Noise

It is believed to be the consequence of imperfections (such as impurities) in the crystalline structure of semiconductors, thus being the result of deficiencies in the device's construction [4]. Its spectral density is approximately proportional to $1/\sqrt{f}$ [8].

Unlike thermal noise or shot noise, flicker noise has the characteristics of *pink noise*. There is no unambiguous equation to calculate its level and is therefore examined experimentally [7]. Its impact is especially apparent when amplifying low frequencies – such as in audio applications.

The effect of flicker noise on spectral noise density of an operational amplifier is to be seen in Figure 1.1

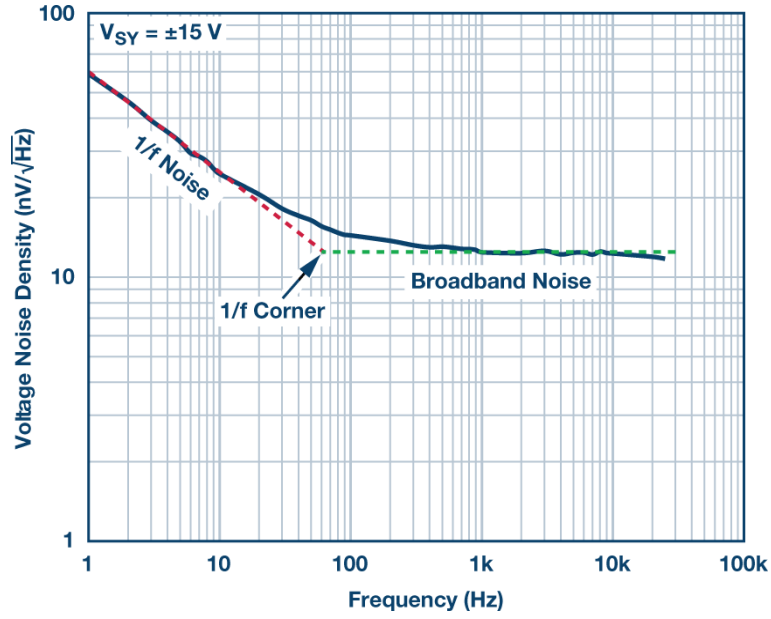


Figure 1.1: ADA4622-2 voltage noise spectral density from [9]

1.2 Distortion

The primary sources of information for this entire section is [7] and [10]. The main parameter determining the amount of distortion in an analog circuit is THD (Total Harmonic Distortion), defined as follows

$$\text{THD} = \frac{\sqrt{\sum_{i=2}^{\infty} U_i^2}}{U_1}, \quad (1.5)$$

where U_i is the RMS value of i -th harmonic component and U_1 is the RMS value of the fundamental harmonic component (which is applied to the input), all of which are measured at the output of an analog circuit. In audio applications it is typically expressed as a percentage, although in communication technology it is more commonly expressed in decibels.

THD is often extended by the level of noise, in that case it is called THD+N and is defined by

$$\text{THD+N} = \frac{\sqrt{U_n^2 + \sum_{i=2}^{\infty} U_i^2}}{U_1}, \quad (1.6)$$

where U_n is the RMS value of noise.

Considering that both THD and THD+N are dependent on several different physical quantities, it is customary that the manufacturers also state the conditions during measurement, such as supply voltage, load impedance or the measured frequency.

Linear forms of distortion (where there are no new frequency components added to the signal), which are namely amplitude and phase distortion [11],

are not to be further examined in this section, as amplitude distortion is often the direct result of amplifying and/or filtering a signal, and phase distortion's audibility is arguable; its impact in audio applications is in most cases therefore negligible.

1.3 Operational Amplifiers

Operational amplifiers (abbreviated Op Amps) are an integral part of many analog circuits. Their parameters come close to an ideal differential amplifier, as they amplify the difference between the two voltages applied to their inverting and non-inverting input [12].

Real operational amplifiers have numerous imperfections which differentiate them from the ideal ones. Their error parameters can be divided into static, dynamic and noise parameters. The main sources of information for the following paragraphs are [8] and [13].

Among the most important static error parameters are finite differential gain A_d , non-zero input offset voltage U_{os} and non-zero input currents I_b , all of which are to be seen in Figure 1.2.

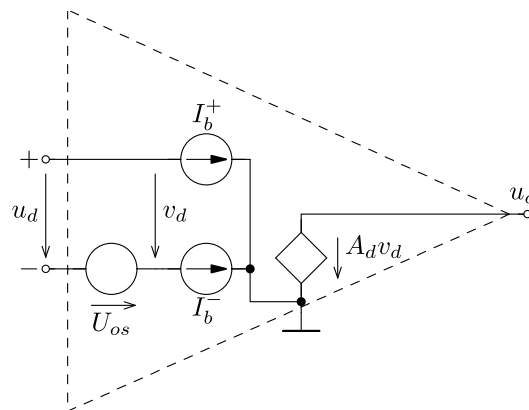


Figure 1.2: Equivalent circuit of an operational amplifier with static error parameters from [13], p. 6 (XII-6/39)

Given that both input offset voltage and input currents will cause a DC error at the output, neither of them are a fundamental parameter when working with audio signals, as often only the AC component is of interest².

Finite differential gain will cause an error in the amplifier's gain A_u . For a non-inverting wiring of an Op Amp, the resulting gain is according to [13] equal to

$$A_u = \frac{A_{uid}}{1 + \frac{A_{uid}}{A_d}}, \quad (1.7)$$

where A_{uid} is the amplifier's ideal gain.

²although a DC offset at the output may reduce the Op Amp's available headroom

Common Mode Rejection Ratio (CMRR) expresses the ratio between differential gain and common mode gain. Thus

$$\text{CMRR} = \frac{A_d}{A_c}. \quad (1.8)$$

In an ideal case it is close to infinity, as the differential gain of an ideal Op Amp is infinite. CMRR has no direct effect on noise or distortion, although high CMRR will lead to better suppression of interference in an audio signal when processing a balanced signal and is therefore a crucial parameter for high-end audio applications. Large common mode voltage at the inputs can lead to distortion at the output [4].

Dynamic parameters of operational amplifiers are time and frequency dependent. Among the most important frequency dependent parameter is the amplifier's differential gain, which will decrease with increasing frequency, and *slew rate*, which is the maximum change of output voltage over time.

The differential gain will typically decrease by 20 dB per decade, where f_0 is the cut-off frequency, at which the gain decreases by 3 dB, and f_t is the transit frequency, where the gain reaches 0 dB.

Slew rate is typically expressed in V/ μ s, and it can lead to significant distortion as can be seen in Figure 1.3.

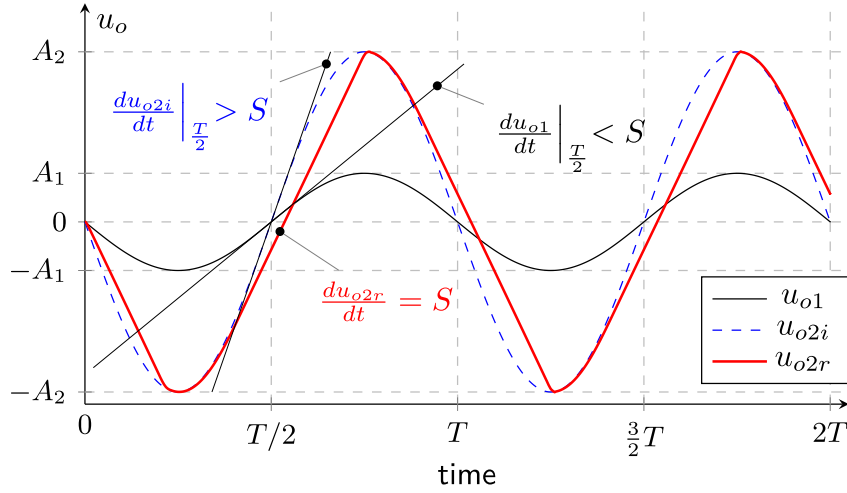


Figure 1.3: Impact of finite slew rate on Op Amp's output signal u_{o2r} from [13], p. 25 (XII-25/39)

The required slew rate S of an Op Amp to output a signal with an amplitude of A_m and a corresponding maximum frequency of f_p is according to [13] defined as

$$S \geq 2\pi A_m f_p. \quad (1.9)$$

Considering that operational amplifiers consist of multiple transistors and are often used with a feedback loop with resistors, all types of noise which were described in Section 1.1 are usually present when using an operational amplifier in a circuit.

Operational amplifiers fitted for audio applications typically use bipolar technology, which opposed to FET technology usually introduces lower voltage noise, while causing higher voltage offset and input currents. JFET input stage might be used to decrease the voltage offset and input currents. According to [8] the Op Amp's noise properties depend mainly on their input stage as after the initial amplification in the input stage the noise contribution of the subsequent stages is insignificant. Furthermore, bipolar Op Amps are more suitable for amplifying signals from low resistance sources as they have higher current noise than FET Op Amps.

Among other requirements for Op Amps are high common mode input and output voltage range (ideally *rail-to-rail*) and low distortion, even with high common mode voltage and low output load. A typical example of an audio-fitted Op Amp is e.g. NE5532/5534, TL072 or AD797 [4].

1.4 Microphones

Since the designed system is expected to have a microphone input and support different types of microphones, basic principles of a microphone and its different types are to be described here in order to provide a theoretical background for the decisions and steps made throughout the designing of the device's analog front-end. The primary source of information for this entire section is [14].

A microphone is a transducer which converts sound pressure to voltage. An ideal microphone will respond purely to sound pressure, although real microphones exhibit some directionality and thus have different response based on the placement of the sound source.

1.4.1 Condenser Microphone

Also referred to as a *capacitor* microphone, condenser microphone works on the principle of a plate capacitor, where one plate is the diaphragm moving with the alternating sound pressure and the other plate (i.e. backplate) is stationary.

The capacitance of a plate capacitor is according to [12] equal to

$$C = \frac{\epsilon_r \epsilon_0 A}{d}, \quad (1.10)$$

where ϵ_0 is the vacuum permittivity, A is the area of overlapping plates, d is the distance between the two plates and ϵ_r is the relative permittivity of the used dielectric. If we also consider that the voltage across a capacitor is as stated in [14] equal to the charge on the capacitor's plates Q divided by the capacity C (see Equation 1.11)

$$U = \frac{Q}{C}, \quad (1.11)$$

Electret microphones therefore do not require polarization voltage but they do require a small power supply voltage for an integrated preamplifier which is usually built into the microphone and which is on a FET transistor basis.

The miniaturization of electret microphones led to them being used in a wide variety of close-in applications such as lavalier hands-free microphones or in mobile or other small electronic devices.

■ 1.4.3 Dynamic Microphone

Also *electrodynamic* or *moving coil* microphone, a dynamic microphone functions on the principle of electromagnetic induction, where a coil attached to the diaphragm is moving in a permanent magnetic field thereby inducing an alternating voltage.

Although dynamic microphones require no DC voltage, they are the least sensitive of all the types mentioned above and therefore require much larger gain.

Chapter 2

Digitization of Audio Signals

Signal processing and transmission of audio signals is over time being increasingly done using digital circuits while the analog ones are being pushed more and more towards the input and output peripheries of electronic devices, as it is mentioned in [16].

The reasons for that are according to [6] namely a much broader range of possibilities of DSP when compared to traditional analog signal processing, much larger immunity to interference and in general lower requirements for preservation of signal waveform over a transmission path, which among other things, allows the transmission of an audio signal over much longer distances and in the vicinity of sources of interference without the loss of information.

As further mentioned in [16], it has therefore become common to integrate the A/D converters into the sensors themselves (i.e. transducers from a non-electrical quantity to an electrical one – in our case a microphone). In that case the whole signal path is purely digital. Otherwise when working with analog sensors it is the designer's task to select a suitable analog-to-digital conversion method for a given application.

The process of digitization of analog signals comprises of sampling (discretization in time), quantization (discretization in amplitude) and coding (expressing the obtained values in a digital form) [8], all of which are to be examined in the following sections.

2.1 Sampling

The primary source of information for this entire section is [8], [7] and [17]. Sampling in the time domain is to be seen in Figure 2.1. The signal values are taken at regular time intervals (i.e. *equidistant* sampling), where T_s is the sample period and $f_s = 1/T_s$ is the sampling frequency or sample rate.

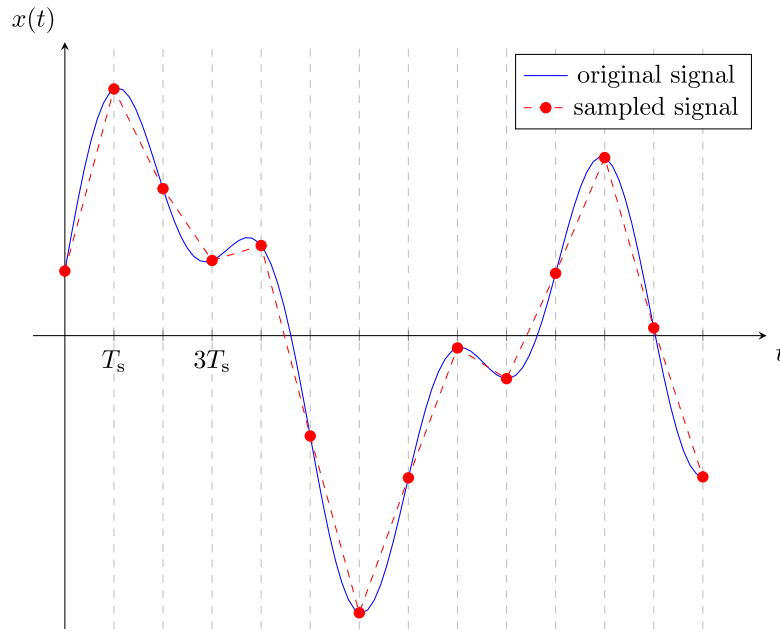


Figure 2.1: Sampling in the time domain

Figure 2.2 shows the spectra of the original and the sampled signal – $X_o(f)$ and $X_s(f)$ respectively. As can be seen, the spectrum of the original signal is copied and mirrored around integer factors of the sample rate, creating side-bands that are an inherent product of sampling. The original signal can therefore be reconstructed from the sampled one with a simple low-pass filter.

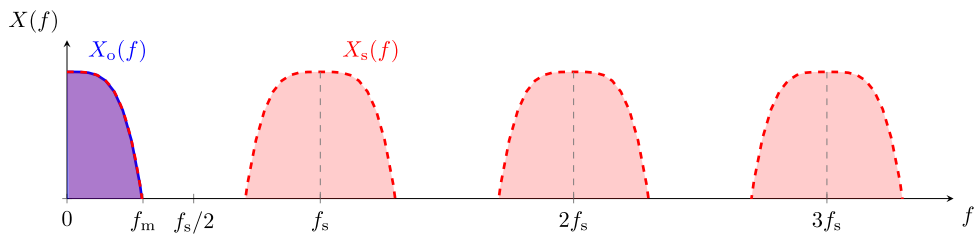


Figure 2.2: Sampling in the spectral domain for $f_s/2 > f_m$

The *Nyquist–Shannon* sample theorem specifies a sufficient condition for a signal to be successfully sampled without the loss of information. For the theorem to hold, the sampled signal must have no energy above f_m , which is considered to be the signal’s maximum frequency, and it must be ensured that

$$f_s > 2f_m. \tag{2.1}$$

For a sample rate f_s which meets the condition above, $f_s/2$ is referred to as the *Nyquist* frequency. Figure 2.3 shows the overlapping spectra for a case in which the sampling condition is not met and aliasing occurs, causing a loss of information.

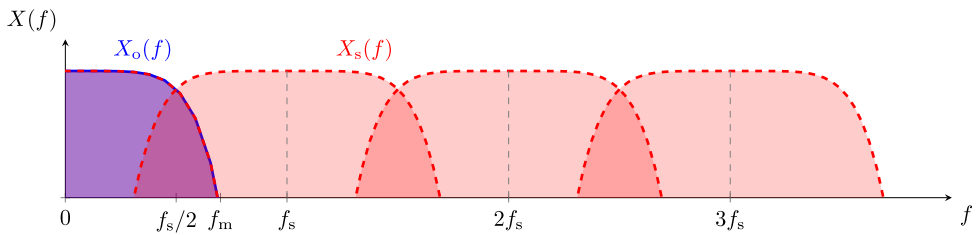


Figure 2.3: Sampling in the spectral domain for $f_s/2 < f_m$

A special case of equidistant sampling is the so-called *band-pass* sampling (or *undersampling*), which allows to sample a band signal with a frequency below the Nyquist frequency, with the use of the free low frequency bandwidth. Non-equidistant sampling includes e.g. *equivalent* sampling, *random* sampling or *adaptive* sampling.

2.2 Quantization

The main source of information for this entire section is [7] and [8]. Figure 2.4 shows a uniform 3-bit quantization of the same signal that was examined in Section 2.1 about sampling.

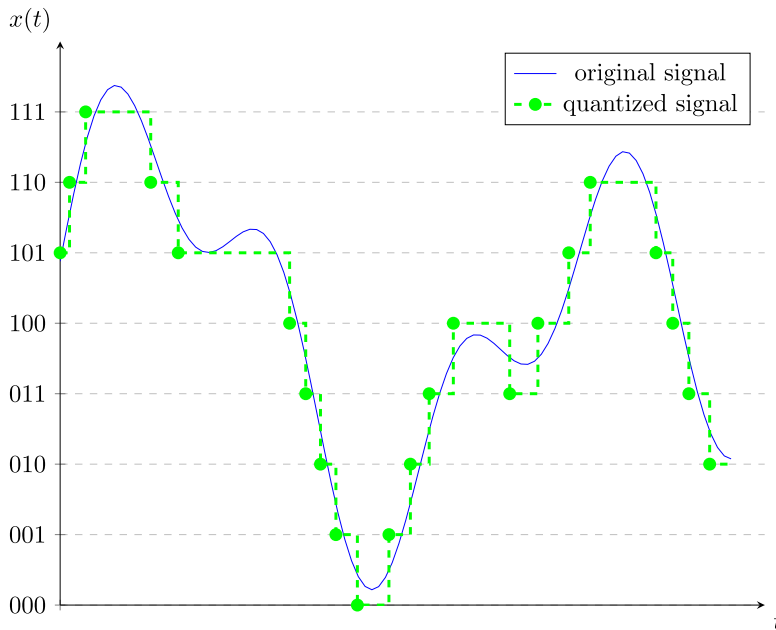


Figure 2.4: Quantization in the time domain

For an n -bit quantization there are 2^n quantization levels, which are all the possible discrete values the quantized signal can acquire. The normalized quantization step q is equal to

$$q = 2^{-n}, \tag{2.2}$$

and it is the smallest difference between two values that the quantizer can distinguish. In practice, to obtain the quantization step as a voltage value, q must be multiplied by the converter's voltage range.

The difference between the real and the quantized value is called *quantization error* or *quantization noise* and it is a function of time having a somewhat random character. Therefore

$$x_q(t) = x(t) + e(t), \quad (2.3)$$

where $x_q(t)$ is the quantized signal, $x(t)$ is the original signal and $e(t)$ is the quantization error.

According to [7], the power spectral density of quantization noise is evenly distributed between 0 and $f_s/2$ and its power remains constant for a given resolution with no regard to the sampling frequency. Hence to reduce the effect of quantization noise, *oversampling* (i.e. sampling at a rate much higher than the Nyquist frequency) is often used, as the noise is then spread out across a wider bandwidth and any noise above f_m can be filtered out. The principle of oversampling is to be seen in Figure 2.5.

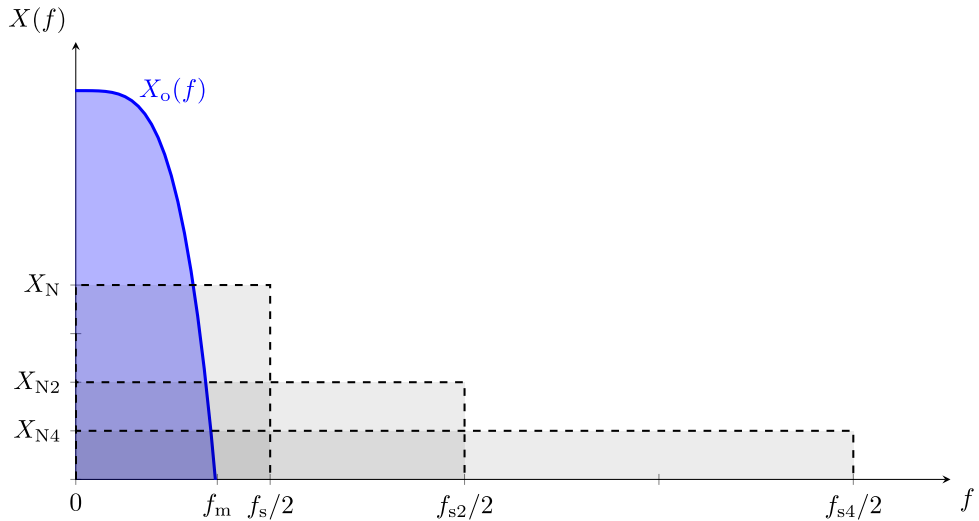


Figure 2.5: Quantization noise spectral distribution for $f_{s4} = 2f_{s2} = 4f_s$

Oversampling is a common technique used in audio applications to increase the converter's dynamic range and SNR. Additionally, as stated in [4], oversampling technology made the use of high order low-pass anti-aliasing filters in front of A/D converters unnecessary, as with higher f_s lower order filters that are generally easier to implement can be used which had a huge impact on the production cost of digital interfaces.

■ 2.3 Coding

Most typically, *binary coding* will be used to encode the quantized samples of a digitized signal. For an n -bit resolution that means that a digital word will have the form of a PCM bit sequence of length n , whereby

$$W = \sum_{i=1}^n a_i 2^{n-i}, \quad (2.4)$$

where W is the digital word value acquiring values from 0 to $2^n - 1$ for the converter's minimum and maximum value, a_1 is the MSB and a_n is the LSB.

Less commonly, *BCD coding* will be used to represent each digit of the decimal form of the obtained quantized sample with a 4-bit sequence. The main source of information for this section was [8].

■ 2.4 Delta-Sigma Converters

The *delta-sigma* or $\Delta\Sigma$ converters, the name of which comes from the meaning of the Greek letters Δ for *difference* and Σ for *sum* [7], are the most commonly used type of ADC's and DAC's in audio application due to their accuracy and suitability for low frequency signals. Delta-sigma converters utilize the delta-sigma modulation, whose principle will be outlined in the following section.

■ 2.4.1 Delta-Sigma Modulation

The modulator's simplified schematic is to be seen in Figure 2.6. The leftmost Op Amp is a summing integrator, where one of the inputs is the analog voltage (V_{in}) and the other input is the feedback comparator essentially working as a 1-bit DAC. The subsequent Op Amp is also a comparator working as a 1-bit ADC and it is followed by a D-type flip-flop circuit synchronizing the output with the clock signal. The feedback comparator is transforming the ground referenced output signal to a ground centered symmetrical signal swinging from $+V$ to $-V$. The schematic and its description is taken from [18].

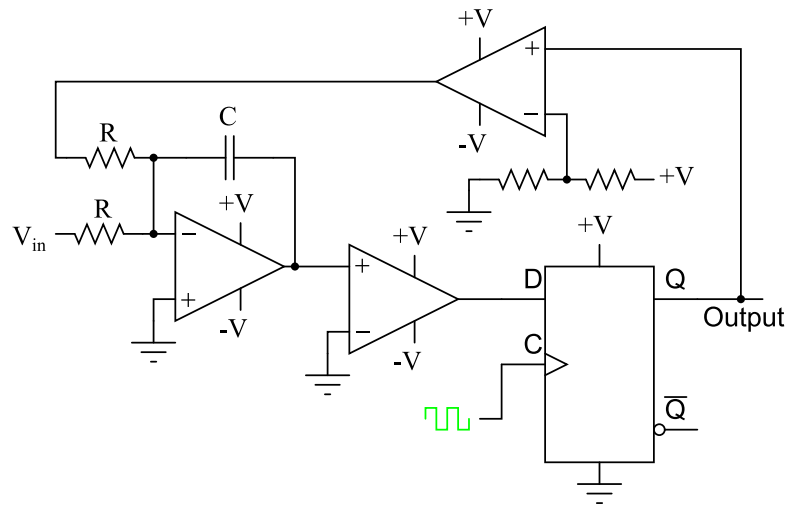


Figure 2.6: Delta sigma modulator simplified schematic from [18], p. 425

As stated in [18]:

"As the analog input signal increases in magnitude, so does the occurrence of 1's in the digital output of the flip-flop" (Kuphaldt [18], 2007, p. 427).

By averaging the output bit stream (in other words retrieving the ratio of 1's and 0's) we can thereby obtain the analog input value. To further process the signal digitally, a counter could be placed after the flip-flop to elaborate the number of 1's for a given number of clock pulses, and some logic included to then convert and store the values in a binary form.

2.4.2 Delta-Sigma A/D Converters

The main source of information for this section is [19] along with [8].

Delta-sigma ADCs utilize the oversampling method with a delta-sigma modulator followed by a low-pass digital filter (i.e. *decimation* filter), removing the excess bandwidth along with the out-of-band noise, and a decimation block, reducing the sampling frequency to one of the standard nominal values used in audio applications (e.g. 44.1 kHz, 48 kHz, 96 kHz, 192 kHz etc.), thereby averaging multiple samples accumulated over time. Figure 2.7 shows the delta-sigma ADC block diagram.

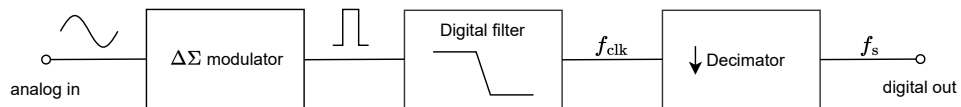


Figure 2.7: The delta-sigma ADC block diagram based on the contents of [19]

The integrator used in the delta-sigma modulator shapes the quantization noise into higher frequencies in addition to the initial noise shaping as a result of the oversampling alone, which further improves the converter's performance

in low frequency high resolution application. Multiple integration stages can be used for extra noise shaping.

2.4.3 Delta-Sigma D/A Converters

The delta-sigma DAC block diagram is to be seen in Figure 2.8. It comprises of an interpolation block, which multiplies the signal's sampling frequency with an oversampling factor k , followed by a low pass digital filter (i.e. *interpolation filter*). The signal then enters a digital delta-sigma modulator connected to a 1-bit DAC, which makes the modulator's output ground centered, swinging from the positive power supply voltage to the negative power supply voltage. Finally, the analog low pass filter then smoothens out the signal to obtain an analog output. The primary information source for the block diagram and its description is [20] and [8].

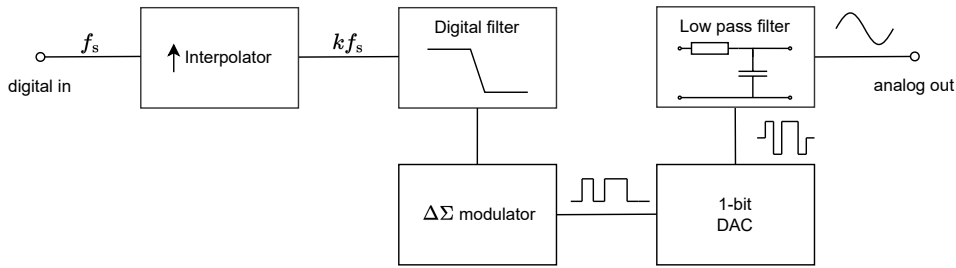


Figure 2.8: The delta-sigma DAC block diagram based on the contents of [20]

According to [21], an alternative to a delta-sigma DAC would be a PWM (Pulse-Width Modulation) DAC. PWM runs on a constant frequency and is more susceptible to duty cycle inaccuracy, whereas in a delta-sigma DAC the duty cycle is constant. Delta-sigma on the other hand requires higher clock rates and generally has a lower bandwidth than PWM, which in the case of audio applications, however, shouldn't be a limitation.

2.4.4 Digital Filters

Since digital filters are an essential part of delta-sigma converters, their principle will be outlined here to provide a basic overview especially with regard to their importance in Part II of this thesis. The main source of information for this entire section is [6].

There are essentially two types of digital filters, an IIR (Infinite Impulse Response) and an FIR (Finite Impulse Response) filters. The Z-transform of the transfer function of an IIR filter has the following general form

$$H(z) = \frac{\sum_{k=0}^M b_k z^{-k}}{\sum_{k=1}^N a_k z^{-k}}, \quad (2.5)$$

whereas in case of an FIR filter the general form is

$$H(z) = \sum_{k=0}^M b_k z^{-k}. \quad (2.6)$$

Both types of filters and their properties will be described in the following sections.

■ IIR

IIR filter output is concluded from the weighted past and present input and past output values as can be seen in the difference equation

$$y[n] = \sum_{k=0}^M b_k x[n-k] - \sum_{k=1}^N a_k y[n-k], \quad (2.7)$$

where $y[n]$ is the output, $x[n]$ is the input and n is the discrete time. Due to the established closed-loop feedback, IIR filters have, as their name suggests, an infinite impulse response similarly to analog filters, and same as in case of analog filters they can be unstable and oscillate at certain frequencies. Additionally, their non-linear phase response is a cause for phase distortion, as the group delay is not frequency independent.

They can, however, achieve better selectivity with lower order than in case of FIR and are therefore the preferred choice whenever the magnitude response is the main concern.

■ FIR

FIR filters have an output concluded purely from the present and past input values weighted by coefficients b_k . Their impulse response therefore has a finite length, as the difference equation

$$y[n] = \sum_{k=0}^N b_k x[n-k] \quad (2.8)$$

gives that

$$h[k] = b_k, \quad (2.9)$$

where $h[k]$ is the impulse response. FIR filters have a linear phase response, which means their group delay is constant and therefore there is no phase distortion occurring. As they do not use closed-loop feedback, they are always stable.

They do on the other hand require higher orders to achieve the same selectivity as IIR filters, due to which they are more computationally demanding and introduce a higher latency.

2.5 Serial Protocols for Digital Audio Transmission

For the so-called *Inter-IC* communication, which is a communication in between integrated circuits on a printed circuit board, typically one of these three serial protocols will be used: *I²S*, *TDM* and *PDM*, all of which will be examined in more detail in the following sections. The main source of information for all three sections is [16] and [22].

2.5.1 I²S

I²S (read as "I-squared-S" or "I-two-S", from Inter-IC Sound) is the most common protocol for the transmission of digital audio in between ICs. I²S is integrated within most modern day A/D and D/A converters as well as many microcontrollers and DSP units.

I²S uses three parallel signal lines to transmit data – the so-called BCK (Bit Clock), LRCK (Left-Right Clock) and SD (Serial Data)¹. The source of the clock signals can be either the transmitter or the receiver or possibly an external clock source can be used.

As can be seen in Figure 2.9, one bit of data is transmitted over the SD data signal line per one clock cycle on the BCK clock signal line while an entire word is transmitted per one clock cycle on the LRCK clock signal line (sometimes called WS - Word Select), which in case of stereo audio transmission chooses between the left and right channel and its frequency is equal to the audio's sampling frequency. The word length is n bits for an n -bit sample resolution (i.e. the number of bits per sample).

I²S then recognizes two of its own variations, a left-justified (LJ) and right-justified (RJ), the two of which vary in the alignment of words on the SD signal line and the polarity of the LRCK clock signal. LJ differentiates from a regular I²S by a one clock cycle data shift on the SD signal line.

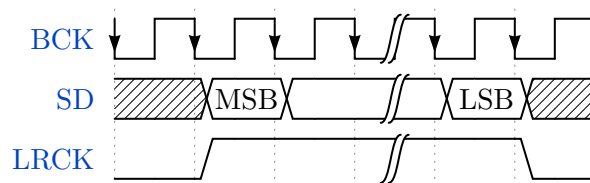


Figure 2.9: I²S signal waveforms based on the contents of [16]

2.5.2 TDM

TDM (from Time Division Multiplex) implements a way to transmit up to sixteen individual channels simultaneously over a single data line (unlike I²S, which is limited to only two channels). Its channel synchronization is done on the FSYNC signal line, where the rising edge usually signals the beginning

¹the names of these signals may vary by manufacturer, though their function remains the same

of an entire data frame. Apart from the above, TDM has a similar working principle as I²S. Its signal waveforms are to be seen in Figure 2.10.

A data frame can be made up of up to sixteen words – in that case every device connected to the TDM bus takes up one sixteenth of the data frame. Thanks to its large channel capacity, TDM is suitable e.g. for a microphone array operation.

TDM isn't as heavily standardized as I²S and different occurrences of this format can have slight variations in its implementation depending on the manufacturer.

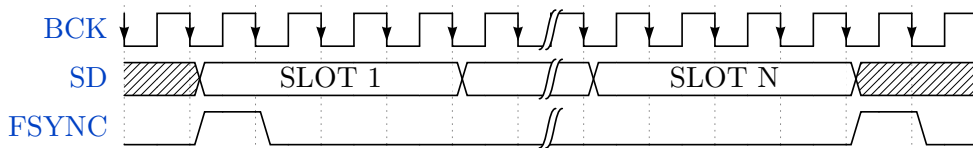


Figure 2.10: TDM signal waveforms based on the contents of [16]

2.5.3 PDM

PDM (from Pulse-Density Modulation) allows for up to two transmitters connected to a single receiver, which generates the clock signal. The transmitters react to opposite clock edges and thereby synchronize their activity.

Unlike TDM and I²S which both use PCM (Pulse-Code Modulation) for encoding words of data, PDM is essentially the direct representation of the analog signal, where the density of 1-bit square wave pulses represents the signal's amplitude – it is in fact the direct output of a delta-sigma modulator which was described in Section 2.4.1.

This data format will most commonly find its use in small mobile electronics such as in cellphones and tablets where it is necessary to route audio signals in the vicinity of sources of EMI (LCD screens, antennas), and where there is a strong emphasis on miniaturization of A/D converters.

Chapter 3

Optical Communication

All the information and equations included in this Chapter are retrieved from [23]. The diagrams are original but based on the contents of [23].

As the advantages of an optical fiber over metallic wiring were already examined in the Introduction of this thesis, this Chapter aims to briefly cover the principles of optical transmitters, receivers and fiber optic cables, as together they create the transmission path of an optical communication system. A principle diagram of an optical communication system is to be seen in Figure 3.1.

The subject of interest in this chapter is the so-called guided optical communication system, which uses an optical fiber as its communication channel unlike an unguided optical communication system which uses free space.

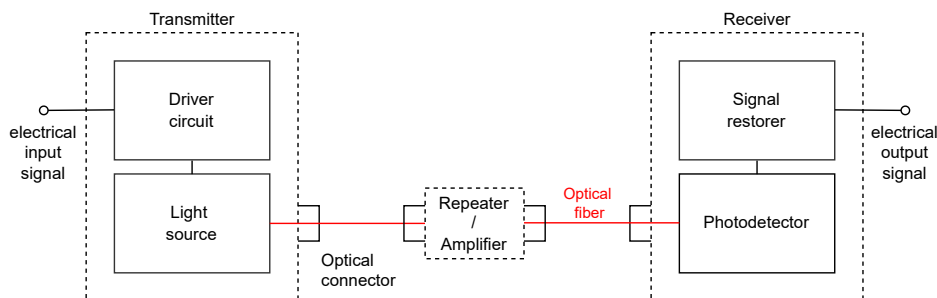


Figure 3.1: A principle diagram of an optical transmission path based on the contents of [23]

The *Driver circuit* is used to drive the *Light source* and/or possibly modulate the signal in a way that is transmittable over an optical fiber. Similarly, the *Signal restorer* block is then used to demodulate the signal from the *Photodetector* to output an electrical signal equivalent to the one at transmitter's electrical input.

The *Repeater / Amplifier* block is an optional element in the transmission path which only becomes necessary for longer distance transmissions due to the fiber's attenuation. Most such devices feature their own optical transmitter and receiver, as the signal processing is usually done in the electrical domain

and therefore an optical-to-electrical conversion is needed, although all-optical signal regenerators which work completely in the optical domain also exist.

3.1 Optical Transmitter

An optical transmitter will typically use semiconductor lasers or LEDs as their light source. The optical signal can be generated by modulating the optical carrier wave, however when using a semiconductor light source, it can be driven by a simple time-varying current, which is a more cost-effective solution as it lacks the need for an external modulator.

An important parameter of an optical transmitter is its *launch power*, as it determines the necessary amplifier/repeater spacing on a transmission path. In optical communication technique, power will often be expressed in dBm, which is defined as

$$P_{dBm} = 10 \log \left(\frac{P}{1 \text{ mW}} \right). \quad (3.1)$$

1 mW is therefore equal to 0 dBm and 1 μ W is equal to -30 dBm. LEDs tend to have a lower launch power of around -10 dBm while semiconductor lasers can reach a launch power of up to 10 dBm, thanks to which they are the preferred choice for most optical transmitters. The maximum bit rate of an optical transmitter is often limited by the front-end electronics rather than the light source itself.

3.2 Optical Fiber

Optical fiber serves as a communication channel between the transmitter and the receiver. It consists of a *core* usually made of silica glass, a *cladding* and a *jacket*. The propagation of light through an optical fiber can be described using geometrical optics. The cladding has a lower refractive index than the core and therefore a ray is reflected at the core-cladding interface. A *total internal reflection* occurs for angles of incidence ϕ larger than the *critical angle* ϕ_c , which is defined by

$$\sin \phi_c = n_2/n_1, \quad (3.2)$$

where n_1 is the refractive index of the core and n_2 is the refractive index of the cladding. Total internal reflection is the mechanism behind light confinement through an optical fiber. Figure 3.2 shows the ray's refraction out of the core for $\phi < \phi_c$ and the ray's total internal reflection for $\phi > \phi_c$.

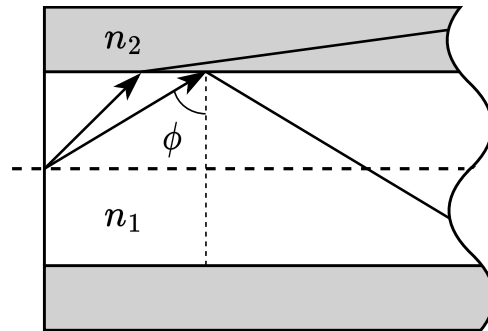


Figure 3.2: Ray refraction and ray reflection in an optical fiber based on the contents of [23]

Silica fibers can have an attenuation as low as 0.2 dB/km. Another important issue of optical fibers is *dispersion*, which mainly occurs in *multi-mode* fibers and which can cause the signal to degrade drastically. *Single-mode* fibers are nearly free of dispersion and are therefore the preferred choice in most applications, although they are more expensive and do exhibit a slight material dispersion, which is related to the frequency dependence of the refractive index.

■ 3.3 Optical Receiver

An optical receiver will typically use photodiodes as its photodetector. Depending on the used modulation, the receiver will feature a dedicated demodulator to restore the original electrical signal. An important parameter of optical receivers is their *sensitivity*, defining the minimum average optical power to fulfill a predetermined BER (Bit Error Rate) requirement. Receiver sensitivity depends mainly on SNR, as there are usually multiple sources of noise present in a receiver, such as shot noise from the photodetectors themselves or thermal noise from the subsequent electronic circuits (see Section 1.1 about noise).



Part II

Practical Part

Chapter 4

Specifications

The assignment is to extend a product line of digital optical converters with a variant capable of transmitting a high quality audio signal. The required parameters for digital audio conversion is a resolution of 24 bits, sample rate of 96 kHz and a frequency response of 20 Hz to 20 kHz \pm 0.3 dB.

The contractor is a company called METEL Ltd, which develops a wide range of security and automation systems finding their use primarily in industrial applications – it is therefore typical to install the company’s products into electrical switchboards or possibly racks, which allows an easy integration of multiple devices into a more complex system.

The device is meant to be used both indoors and outdoors, which brings strict requirements on its functioning temperature range and its resistance to other external conditions such as humidity. The use of all temperature dependent electro-mechanical components (e.g. mechanical switches, potentiometers) which can additionally degrade due to excessive moisture and become unsuitable for conducting signals is therefore undesirable. The control features are also meant to be sturdy and accessible while not getting in the way of other devices when installed in a switchboard.

Two devices are to be produced (a transmitter and a receiver), both of which will be implemented on a single printed circuit board with two different variants of component mounting. The board’s size is to be strictly 100 mm \times 115 mm for a possible insertion into one of the company’s mass-produced aluminium chassis adapted for a switchboard installation (to be seen in Figure 4.1). With regard to the production price only the top side of the board is to be mounted with components and the use of any microcontrollers is unfavorable.

Part of the device incorporating the optical conversion using serializers/deserializers and a Small Form-factor Pluggable (SFP) optical transceiver was developed by the contractor in the past and is under a non-disclosure agreement. Its schematic will therefore not be shown in this thesis and only its basic principle will be outlined.



Figure 4.1: An industrial PLC from the contractor’s IPLOG-GAMA series using the same aluminium chassis as the intended product

Given that the device is expected to transmit only two audio channels and that the serializers/deserializers allow to process and transmit data from several parallel signal lines, the I²S serial protocol (described in Section 2.5.1) comes out as the most convenient choice for the digital audio format, as TDM would be suitable for a transmission of more than two channels and PDM only if transmission over a single data line is necessary, as it requires higher frequencies to achieve the same quality of digital audio and thus results in an increased EMI on the PCB.

4.1 Component Selection

All the components used have a functioning temperature range requirement of -40 °C to 70 °C, suitable for industrial applications. Both the analog and digital circuitry is to have its own dedicated power supply to prevent any unwanted interference in the audio signal.

Since the part of the circuit performing the optical conversion falling into the digital section of the device is powered by a 3.3 V power supply, the same should apply to all the newly selected digital components for compatibility.

Other important parameters are noise and distortion, mainly for components used in the analog section of the device. As the task is to essentially transmit audio of the highest possible quality, no specific limit parameters are given in this area and rather the best price-performance ratio solution is to be implemented.

■ 4.1.1 Capacitors

The choice of capacitors in an audio path is not to be overlooked, as it can have a huge impact on the system's distortion. The article [24] discusses this issue, and recommends the use of electrolytic, tantalum or film capacitors whenever possible, as MLCC¹ capacitors, although they are usually the cheaper and the smallest size option, can degrade the audio signal significantly.

When going for a ceramic capacitor, ideally, first class C0G/NP0 ceramic capacitors are to be used, due to their very good stability. It is however not easy to find such capacitors in values greater than 0.1 μF and they are much more expensive than the second class options such as X7R or X5R capacitors.

Furthermore, in [24] it is stated that:

"It is possible to minimize the distortion from MLCC capacitors by using larger-value capacitors and increasing the load impedance that the capacitor sees." (Kaye [24], 2020, p. 4).

The use of non-ceramic capacitors isn't however always possible, as most of them have a polarized dielectric and therefore require their anode to be kept at a higher voltage than the cathode to prevent the capacitor from being damaged. An exception is the film capacitor, which from all the non-ceramic capacitors usually offers the best performance and is therefore the preferred option.

■ 4.1.2 A/D Converter

The PCM1861 from Texas Instruments was selected as the audio ADC, as it is a hardware controlled 110 dB SNR front-end device allowing for a 24 bit resolution and 96 kHz sample rate conversion as was requested by the contractor. The PCM186x family of audio converters incorporates the I²S serial protocol and it allows separate powering of its analog and digital section, both of which have a recommended voltage value of 3.3 V – therefore all the other components used in the analog section of this device must work off of that same nominal voltage (the digital section was already predetermined to work off that voltage as explained in Section 4.1). [25].

■ 4.1.3 D/A Converter

While being compatible with the above mentioned ADC in terms of digital data format and power parameters, the PCM5102A DAC from Texas Instruments additionally features ground centered stereo output with a 112 dB SNR and a soft-mute capability, also allowing for output loads down to 1 k Ω [26].

¹Multilayer Ceramic Capacitors

4.1.4 Operational Amplifiers

For analog audio processing the TL972 operational amplifier from Texas Instruments was selected especially due to its low operating voltage and, additionally, numerous other parameters, such as low noise and low distortion, as it is explicitly marked as ideal for audio applications by the manufacturer. TL972 also features two Op Amps in a single housing which is suitable for our use [27].

4.1.5 I/O Connectors

The device will feature two audio connectors, allowing for a simultaneous connection of both a microphone (or any balanced audio source) and a stereo line.

XLR combined with 6.3 mm stereo jack connector from Neutrik was selected for a microphone or balanced input on the transmitter's side and a balanced output on the receiver's side (to be seen in Figure 4.2), and a dual cinch connector from CUI was selected for stereo line audio input on the transmitter's side and stereo line audio output on the receiver's side.

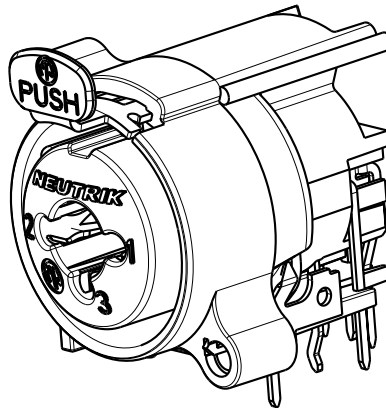


Figure 4.2: NCJ6FA-H: 3 pole XLR female receptacle with 6.3 mm stereo jack, horizontal PCB mount from [28]

The contractor's optical conversion design uses an SFP connector for fiber-optic cable connection and WR-TBL terminal block connectors for the connection of

- a logical input/output,
- a *lock* logical output which can be used to evaluate externally whether the two devices's optical conversion circuits have synchronized and locked onto one another (i.e. whether the system is transmitting and receiving data),
- a power supply voltage.

4.1.6 Switches

The device's control and setup is to be implemented using dip switches (see Figure 4.3) in combination with electronic analog switches TS3A24157 from Texas Instruments, which are a two-channel SPDT switches with a low ON-state resistance of $0.65\text{ m}\Omega$ fitted for audio applications [29]. For higher voltages such as in case of phantom power, relays are to be used instead – namely G5V-1 from Omron, as TS3A24157 can only handle a maximum voltage of 3.6 V .

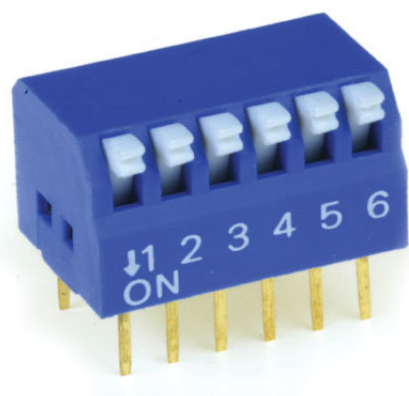


Figure 4.3: D4006RP dip switch from OMEGA FUSIBILI commonly used by the contractor

4.1.7 Clock

The ADC requires a clock of 49.152 MHz to set the required sampling frequency – the clock serves as the oversampling rate in the delta-sigma modulator and with a decimation factor of 512 the audio sampling frequency is then set to 96 kHz .

A clock oscillator C3391 with such frequency was selected and is to be used along with NC7WZ17 buffers to prevent signal reflections on clock buses. The oscillator is also going to clock the serializer circuits used before the optical conversion on the transmitter's side and the deserializer circuits used on the receiver's side. The DAC doesn't require external clocking as it can derive its own clock from the I²S input.

4.1.8 Power Supply Circuits

All the devices in the contractor's products line function off of a $10\text{ to }60\text{ VDC}$ (or $10\text{ to }36\text{ VAC}$) power supply range. The contractor's optical conversion design is powered by a DC/DC step-down converter TPS54160 from Texas Instruments, capable of supplying up to 1.5 A of current [30], which will be used to supply also the digital section of the audio processing circuits.

For supplying the analog section a linear regulator LT3012B from Linear Technology was selected, especially due to its high range of input voltages

and its availability. The same unit will be used to supply phantom power to the microphone input for condenser microphones – since the use of any step-up DC/DC converter was marked as undesirable by the contractor, the LT3012B will be set to output 48 V while being limited by the input voltage and thus only being able to supply its input voltage reduced by its dropout voltage, which is around 400 mV [31].

Chapter 5

Design

The entire project was designed using *Altium Designer 22*, which is an ECAD software used by the contractor. Segments of the schematic were simulated in *LTSpice*, an open-source electronic simulation software based on SPICE.

5.1 Transmitter

The transmitter's principle block diagram is to be seen in Figure 5.1.

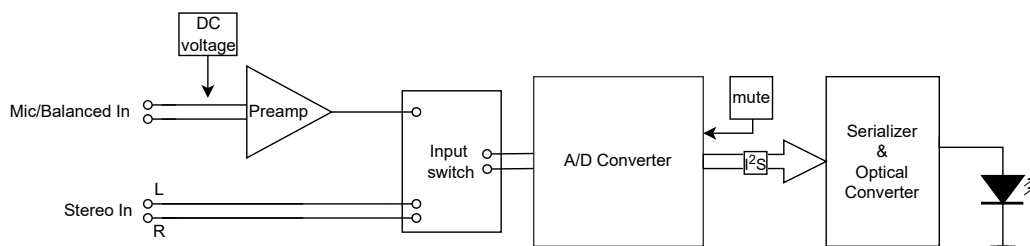


Figure 5.1: The transmitter's principle block diagram

5.1.1 Preamplifier – design

The designed preamplifier consists of two stages, first one being a differential amplifier for processing a differential (balanced) input signal and second one being a non-inverting amplifier with discreetly adjustable gain – see Figure 5.2.

The first stage has matching input resistances for a differential input on the positive and negative input to get a symmetrical load on the XLR connector. Resistor values in the differential stage were at first chosen very high to prevent a low frequency cut-off in combination with input 100 nF C0G ceramic capacitors, the use of which was desirable due to their excellent stability. The resistors turned out to cause an unacceptably high noise and less stable X7R higher capacity capacitors were therefore mounted in combination with lower value resistors to retain the circuit's flat frequency response while lowering the resistor noise contribution. Figure 5.2 shows the updated preamplifier's version. See Section 6.2 in Chapter 6 about testing for further details about this issue.

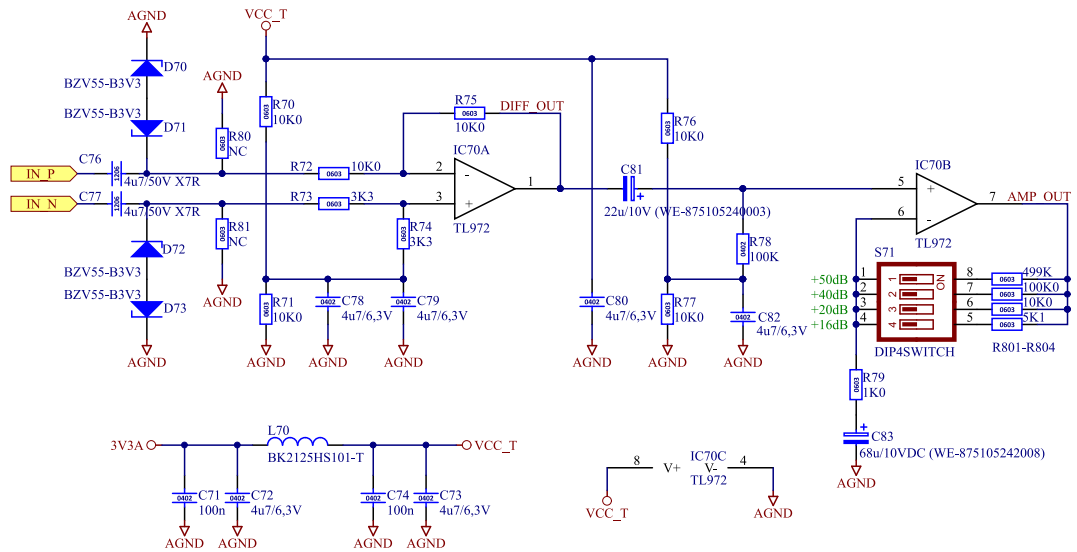


Figure 5.2: Full schematic of the preamplifier

Protective zener diodes were added to prevent potential voltage peaks (which are likely to occur when turning on phantom power) from damaging the Op Amps. The differential amp's function is to be seen in Figure 5.3, where $V(in_p)$ and $V(in_n)$ (the green and blue waveform respectively) are the input signals and $V(diff_out)$ is the differential amplifier's output signal. The second stage features a dip switch which connects feedback resistors in parallel allowing the user to choose from four discrete values of gain. The amplifier's frequency response for a 38 dB gain is to be seen in Figure 5.4.

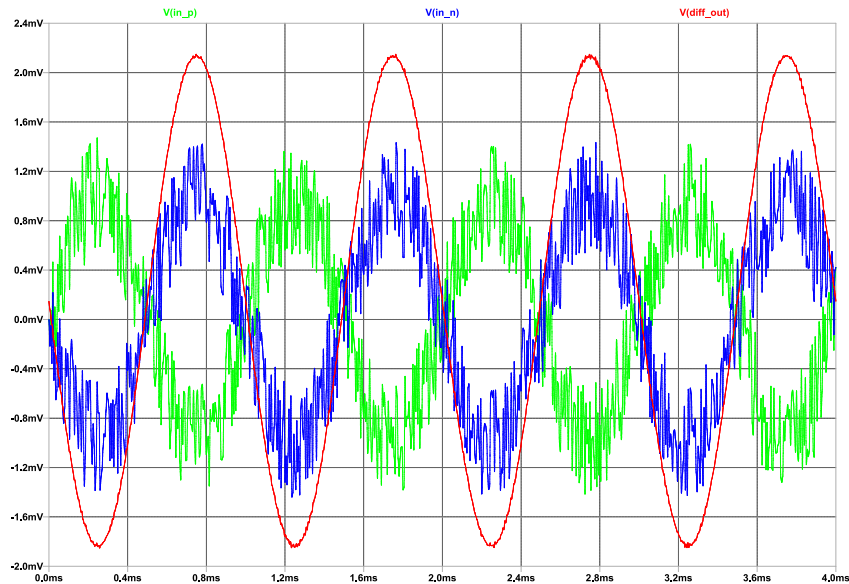


Figure 5.3: Simulated differential amplifier output (with removed DC component from Op Amp bias) for 1 kHz sinusoidal input with added common noise from LTSpice

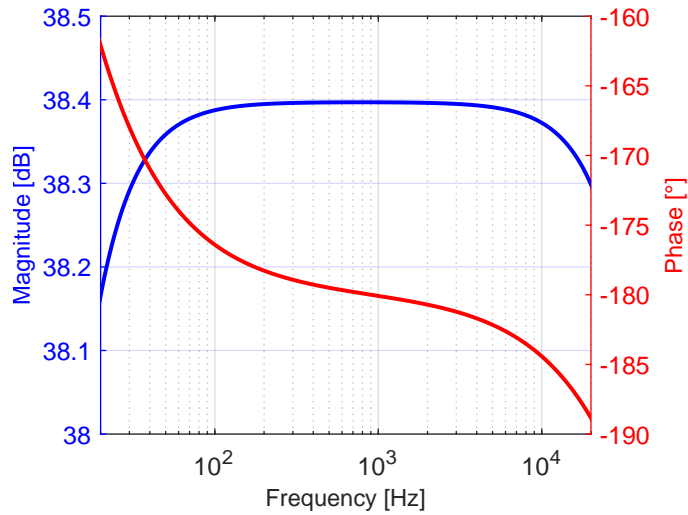


Figure 5.4: Simulated preamplifier's frequency response for a 38 dB gain from LTSpice

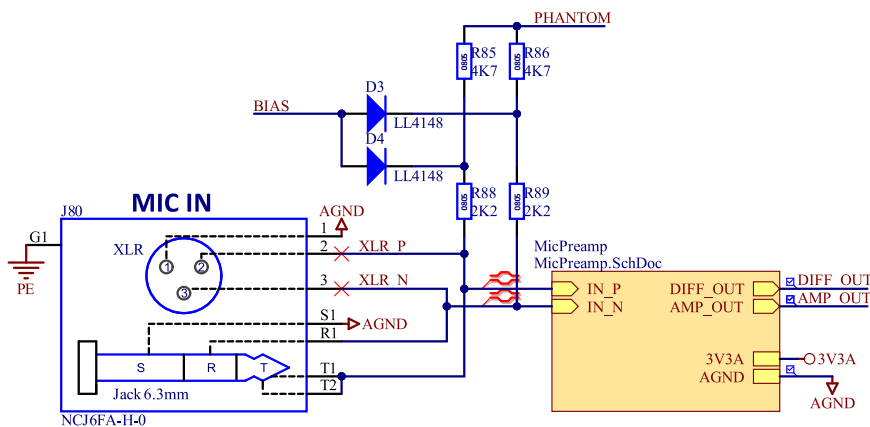


Figure 5.5: Input XLR connection to preamplifier

Figure 5.5 shows the preamplifier's connection to the NCJ6FA-H connector along with the bias wiring. The bias switching will be described in Section 5.3.

5.1.2 A/D Converter – design

The full schematic of the ADC and its accompanying circuits is to be seen in Figure 5.6. Since PCM1861 establishes its own DC bias on the analog inputs, polarized polymer blocking capacitors (C90 & C91) can be used, as they have excellent stability and are therefore suitable for conducting audio signals. The stereo line inputs are brought to the converter's channel one, while the microphone input is brought to the channel four due to switching convenience. Zero resistors (0R0) and unconnected resistors (NC) were used on numerous places to provide further wiring capabilities after the PCB's manufacturing.

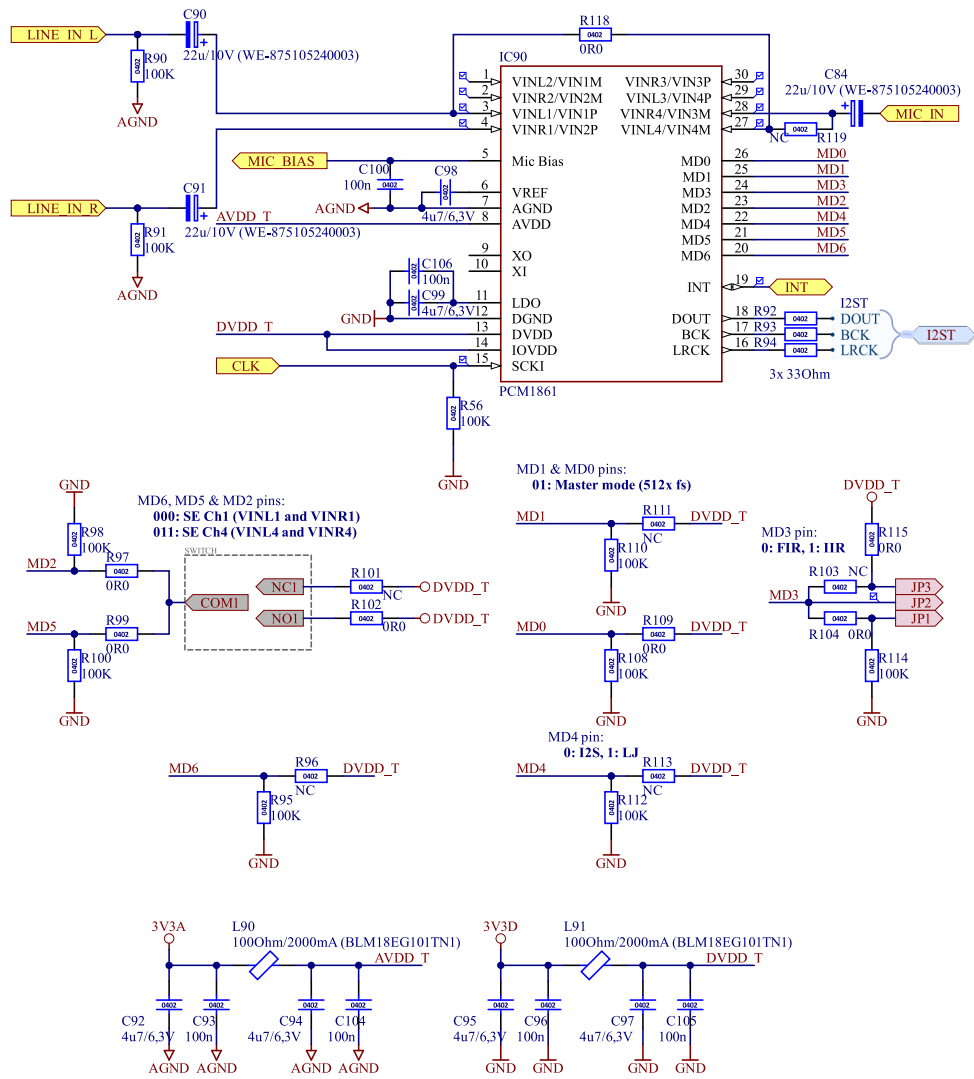


Figure 5.6: A/D converter full schematic

Pins MD0 to MD6 allow for the converter’s control and setup. While pins MD0, MD1 and MD4 are hardwired to set the decimation factor and the digital data format which aren’t meant to be changed during the device’s operation; pins MD6, MD5 and MD2 control the analog multiplexer at the input of the converter (see Figure 5.7) and are therefore controlled by one of the electronic switches placed outside this schematic block to choose either from line or microphone input.

Furthermore, MD3 allows the user to choose from either an IIR or an FIR decimation filter and is to be initially controlled by a jumper until the more fitting choice is chosen during testing and hardwired by changing the resistor mounting.

Although PCM1861 provides capabilities for processing a balanced signal – namely a differential input and a programmable gain amplifier (PGA), its controllability is very limited (as can be seen in Figure 5.7) and its CMRR is typically only 56 dB [25]. The design of a standalone preamplifier was therefore favorable, as it is expected to provide wider range of gain options and offer better suppression of interference, as the TL972 Op Amp has a typical CMRR of 85 dB¹ [27].

Analog MUX and gain selection using MD6, MD5, and MD2 pins, respectively: 000: SE Ch 1 (VINL1 and VINR1) 001: SE Ch 2 (VINL2 and VINR2) 010: SE Ch 3 (VINL3 and VINR3) 011: SE Ch 4 (VINL4 and VINR4) 100: SE Ch 4 with 12-dB gain 101: SE Ch 4 with 32-dB gain 110: Diff Ch 1 (VIN1P and VIN1M, VIN2P and VIN2M) 111: Diff Ch 2 (VIN3P and VIN3M, VIN4P and VIN4M) with 12-dB gain

Figure 5.7: Pin function description for pins MD6, MD5 and MD2 from PCM1861 datasheet [25]

PCM1861 also provides a microphone bias output of 2.6 V which is derived from the analog power supply and which is to be used to bias electret microphones. Pin INT can serve as an interrupt output or as a logical input allowing to mute the audio by setting the data signal line to zero when brought high. After the board’s manufacturing the pin was wired to one of the dip switch’s poles and serves as a mute control since then.

5.2 Receiver

The receiver’s principle block diagram is to be seen in Figure 5.8.

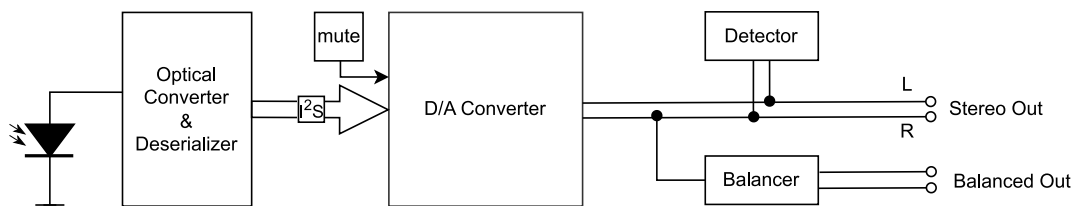


Figure 5.8: The receiver’s principle block diagram

5.2.1 D/A Converter – design

The DAC and its accompanying circuits schematic is to be seen in Figure 5.9. Since PCM5102A features an integrated charge pump inverting its analog supply voltage, the audio outputs (OUTL & OUTR) are ground centered and therefore no decoupling capacitors in the audio path are needed.

¹although according to [4] an Op Amp’s CMRR is only equal to the differential amplifier’s CMRR if all the resistors are matched

The charge pump pins however do require a decoupling and flying capacitor (C128 & C129). An RC lowpass filter is used at the audio outputs based on the manufacturer's recommendation in the datasheet.

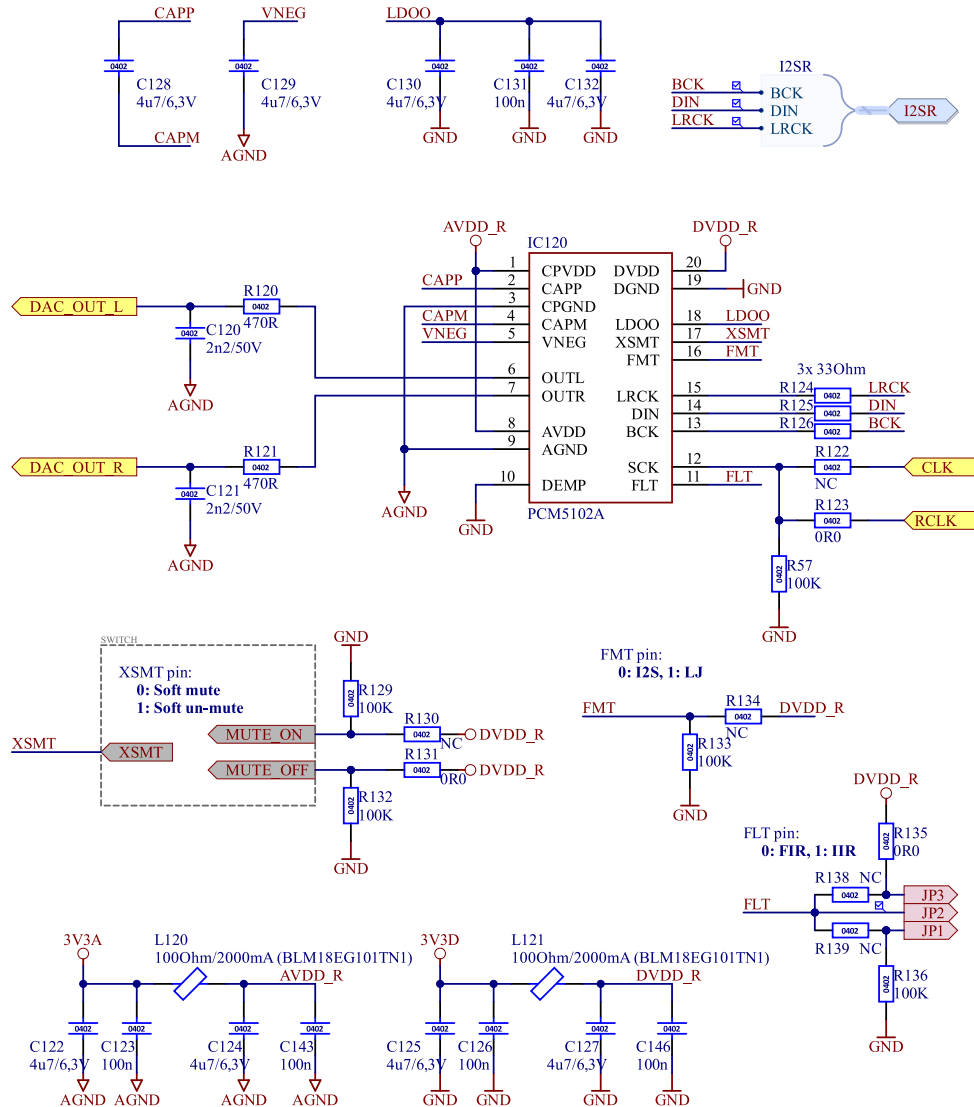


Figure 5.9: Full D/A converter schematic

The device is clocked using the so called recovered clock (RCLK) retrieved from the optical conversion and deserializers circuits, although a regular clock oscillator input (CLK) is brought to the DAC with a not connected resistor R122 for further wiring capabilities. PCM5102A additionally makes the elimination of any system clock (SCK) possible as it can derive the clock from the I²S digital input. Different options of clocking are to be tested after the PCB's manufacturing in case of any issues with the current clock wiring (e.g. clock *jitter* causing distortion to the audio signal).

The FLT pin allows the user to choose from either an FIR or an IIR interpolation filter, and is to be initially controlled by a jumper (the same one as in case of the transmitter's PCM1861 decimation filter) until the more fitting solution is selected and hardwired.

The XSMT pin controls the soft mute and soft un-mute function. When shifted from high to low a soft attenuation ramp begins and when driven from low to high a soft un-mute process begins. This allows mute or un-mute the audio outputs without any unwanted pops or clicks in the audio signal. The pin will be controlled by one of the TS3A24157 switches placed outside this schematic block.

The FMT pin allows to choose from a I²S or a LJ digital input format (see Section 2.5.1 for further details). It is by default hardwired to set the format to I²S.

5.2.2 Audio Balancer – design

This circuit's purpose is to output a balanced audio signal from a single-ended (SE) input. Its full schematic is to be seen in Figure 5.10.

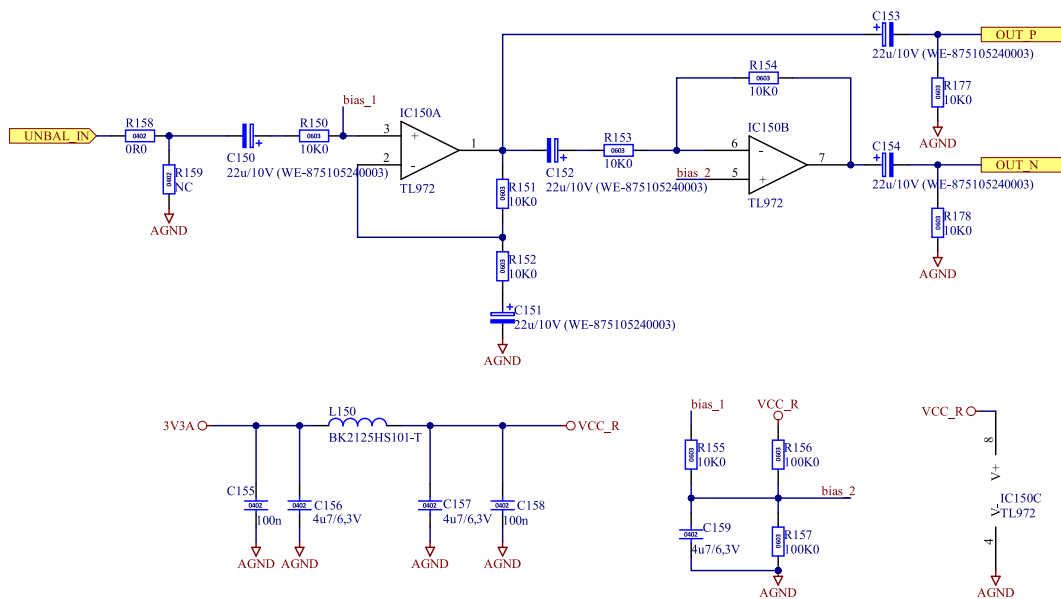


Figure 5.10: Audio balancer schematic

Figure 5.11 shows the transient analysis of input and output signals, where $V(\text{out_p})$ (blue waveform) is the positive channel, $V(\text{out_n})$ (red waveform) is the negative channel and $V(\text{unbal_in})$ (green waveform) is the SE input. Figure 5.12 shows the AC analysis of balancer's output. The gain is approximately 6 dB, as the total balanced output voltage between positive and negative pins is twice the voltage of the unbalanced input as it is mentioned in [4].

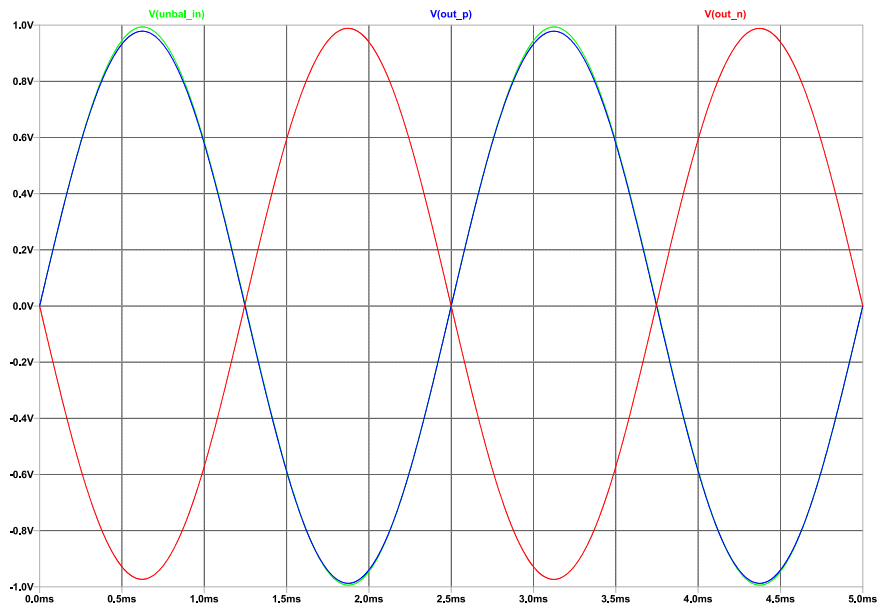


Figure 5.11: Simulated balancer's output signals for a 1kHz sine wave input from LTSpice

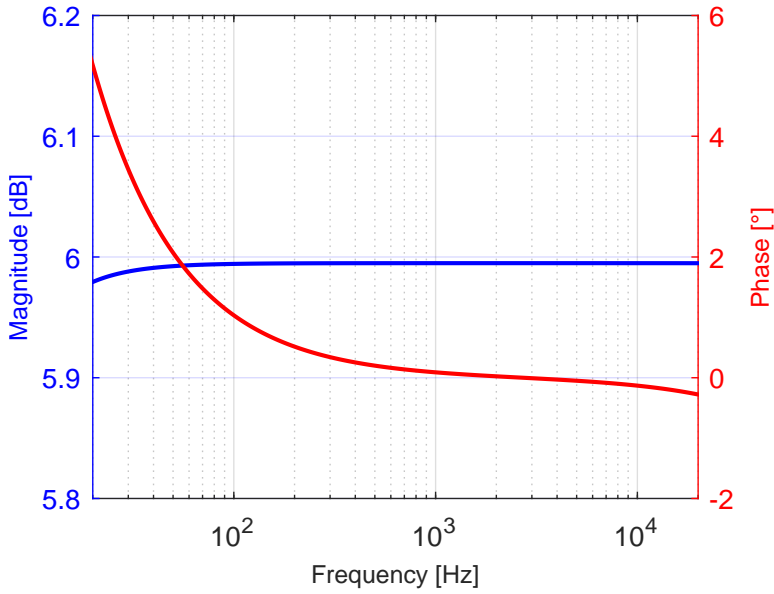


Figure 5.12: Balancer's AC analysis from LTSPice

5.2.3 Audio Detector – design

The audio detector's purpose is to signal an audio signal at the input/output with an LED placed on the device's front panel. Two versions of this circuit were designed and tested and are to be examined in the following sections.

1st version

Figure 5.13 shows the first version of the audio detector circuit. The LED is placed outside this schematic block and is to be modulated by a stereo audio input using two rail-to-rail LM2904 operational amplifiers used as voltage controlled current sources.

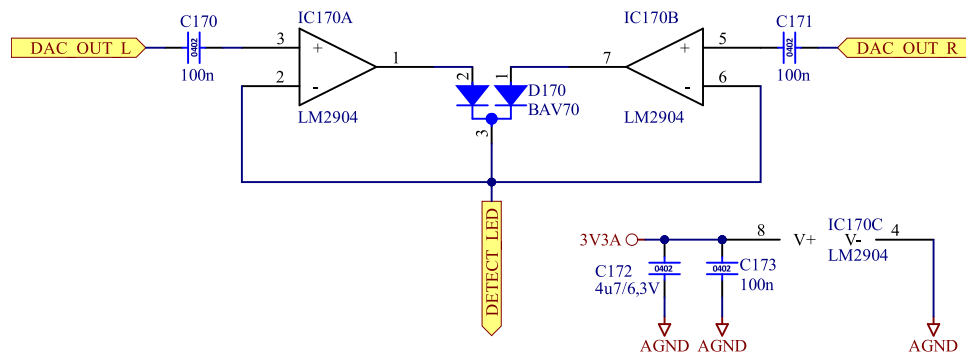


Figure 5.13: Audio detector schematic - 1st version

2nd version

The circuit in Section 5.2.3 was in spite of the simulations performed unfortunately found to be non-functional and therefore a new version was designed and tested. Its schematic is to be seen in Figure 5.14. It was decided that all channels should have their own individual signaling LED. The circuit is not present on the manufactured board but is expected to be built into the next version. The LEDs are lit from around 100 mVpp and their luminosity then somewhat increases with increasing voltage.

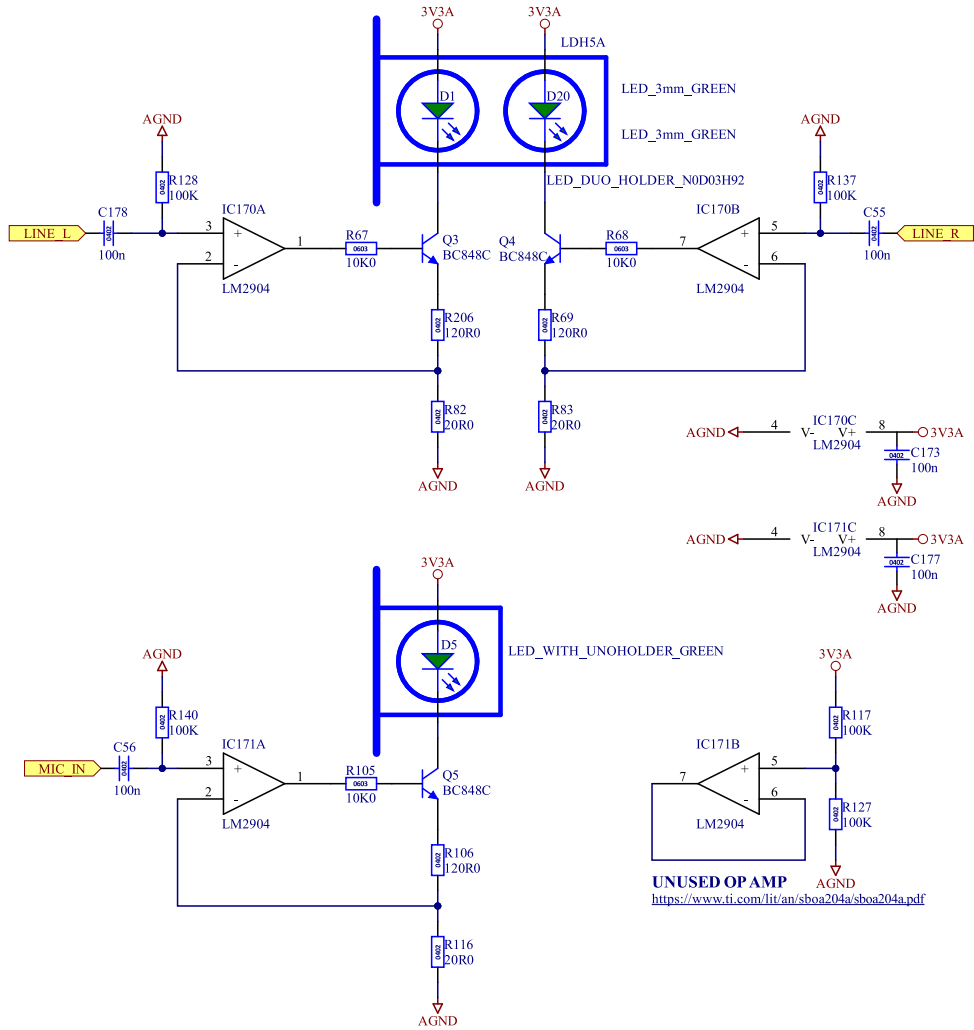


Figure 5.14: Audio detector schematic - 2nd version

5.3 Switching Circuits – design

The switching circuits are controlled using a dip switch which is to be seen in Figure 5.15 along with the jumper which chooses from either an FIR or an IIR decimation/interpolation filter on the transmitter’s or the receiver’s side respectively.

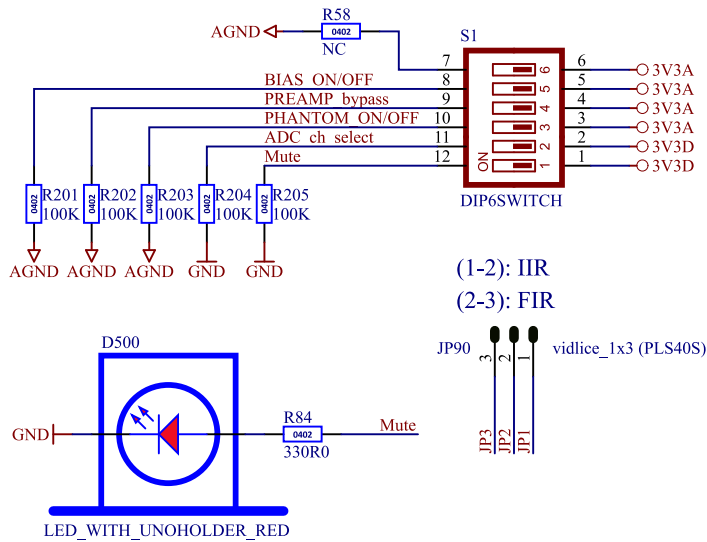


Figure 5.15: Dip switch and jumper schematic

The dip switch connects to two TS3A24157 switches (two poles each), one being used to switch analog and the other one being used to switch digital parts of the circuit – separated to prevent unwanted interference. Their schematic is to be seen in Figure 5.16.

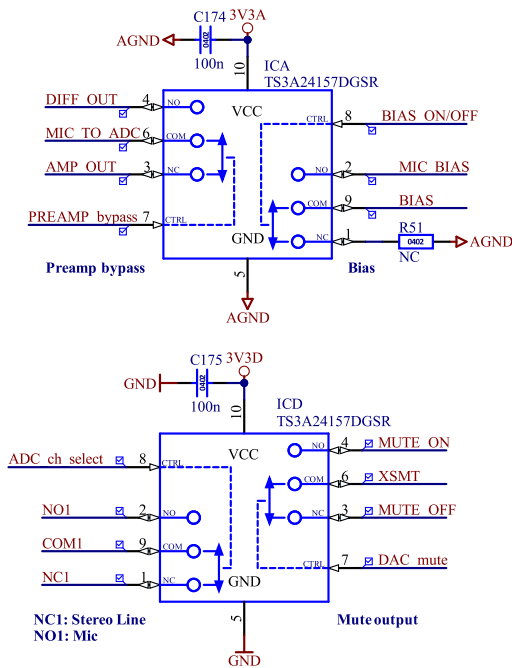


Figure 5.16: TS3A24157 switches schematic

Phantom power is due to high voltage engaged using a relay circuit, which is to be seen in Figure 5.17. The base of Q1 bipolar transistor is connected to one of the dip switch poles through a 1 kΩ resistor.

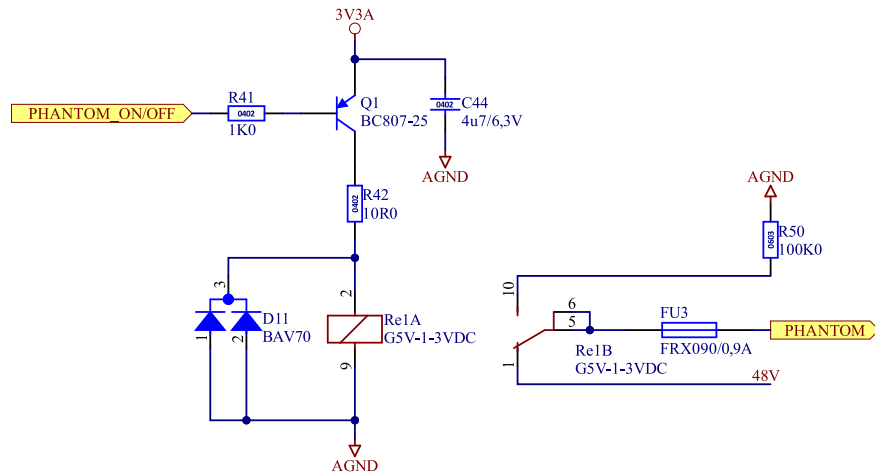


Figure 5.17: Phantom power switching schematic

5.4 Power Supply – design

As was previously mentioned in Section 4.1.8, the device apart from functioning off of a 10 to 60 VDC or a 10 to 36 VAC input power supply range must also have its own dedicated power supplies for its analog and digital section.

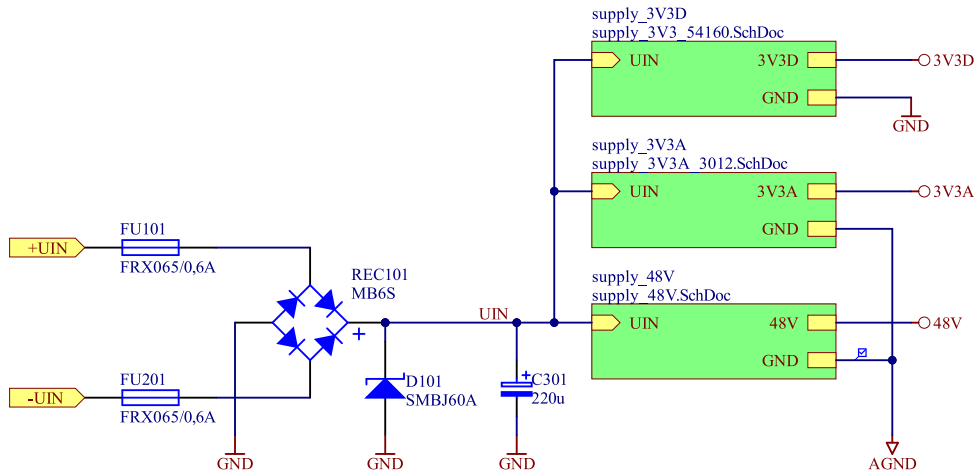


Figure 5.18: Input power supply circuit schematic

While the digital 3.3 V supply circuit was designed by the contractor in the past and incorporates a TPS54160 buck converter capable of supplying up to 1.5 A, the analog power supplies had yet to be designed. The schematic of the analog 3.3 V power supply is to be seen in Figure 5.19. The 48 V power supply schematic is essentially the same only with different resistor values and without the protective schottky diode.

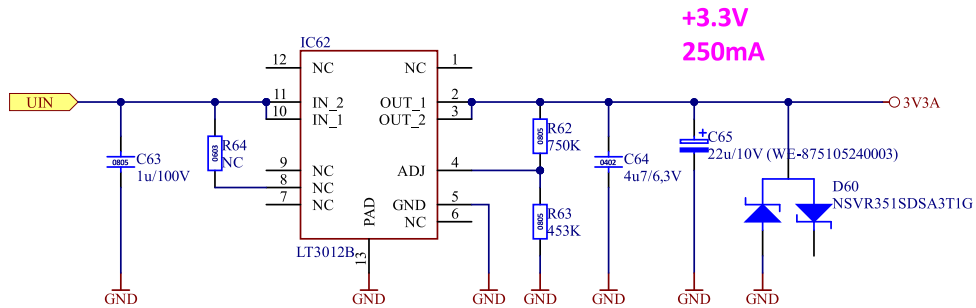


Figure 5.19: Analog 3.3 V power supply schematic with LT3012B

The output voltage is according to the regulator's datasheet [31] equal to:

$$V_{\text{OUT}} = 1.24 \text{ V} \times \left(1 + \frac{R_{62}}{R_{63}} \right) + I_{\text{ADJ}} \times R_{62}, \quad (5.1)$$

where

$$I_{\text{ADJ}} = 30 \text{ nA at } T = 25 \text{ }^\circ\text{C} \quad (5.2)$$

and R_{62} with R_{63} are the corresponding resistor values. The R_{64} not connected resistor is included in the schematic for a possible mounting of one of the related regulators LT3012 or LT3013 from Linear Technology (which additionally feature a shutdown pin) in case of availability problems with the LT3012B regulator used.

5.5 Clock – design

The clock distribution circuit consisting of a clock oscillator CE3391 and two NC7WZ17P6X buffers is to be seen in Figure 5.20. The left buffer clocks the serializer or the deserializer on the transmitter's or the receiver's side respectively. Similarly the right buffer clocks the ADC or the DAC (although the DAC is by default disconnected from the buffer as it uses the recovered clock from the optical conversion as was previously explained in Section 5.2.1).

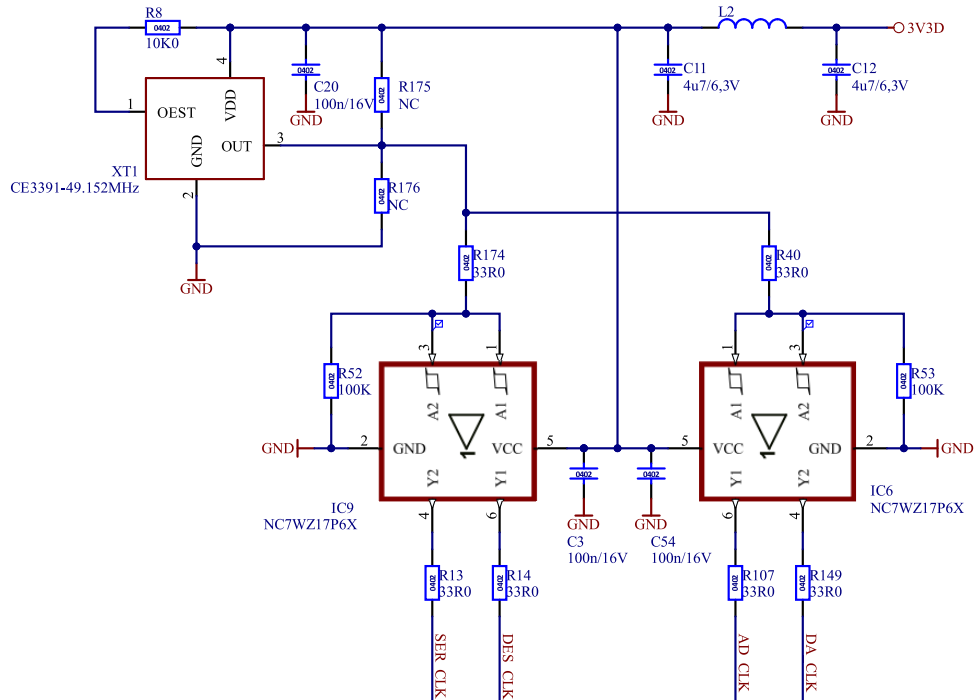


Figure 5.20: The clock distribution circuit schematic

Series resistors are used on the clock lines and are to be placed close to the buffers to prevent clock reflection as well as providing the possibility of disconnecting a component from its clock when its not mounted to prevent the clock's trace from acting as an antenna and increasing EMI. To provide an overview of the two default mounting variants Table 5.1 is included.

Table 5.1: Series resistors on clock lines mounting variants

Resistor	TDW (Transmitter)	RDW (Receiver)
R ₁₃	Mounted	Not Mounted
R ₁₄	Not Mounted	Mounted
R ₁₀₇	Mounted	Not Mounted
R ₁₄₉	Not Mounted	Not Mounted ²

²to be possibly mounted in case of issues with the recovered clock – e.g. clock jitter

5.6 PCB design

Figure 5.21 shows a picture of the designed and manufactured PCB which was at the time yet to be mounted with components. The PCB is a four-layer, mounted only from the top, with its lower half being analog and its upper half being digital. The two grounds are connected with a zero resistor at the board's right side to prevent ground loops of digital circuits from interfering with the analog circuits while also keeping both grounds at the same potential. The ADC and DAC have their analog and digital interfaces at the opposite sides of the package and therefore bridge these two board sections in the middle.

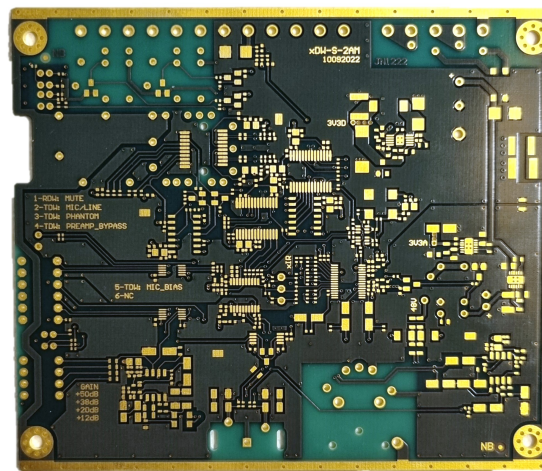


Figure 5.21: The designed unmounted PCB

Both the analog and digital 3.3 V are distributed with polygon planes in the inner bottom layer to prevent voltage drops caused by trace resistance and provide a low impedance path to the components as well as facilitate heat dissipation. Most signal traces are routed in the top layer to maintain signal integrity as the inner top layer is almost entirely comprised of ground planes.

The upper part of the PCB is mounted with WR-TBL terminal block connectors while the lower half with the audio connectors. The left side of the PCB is mounted with panel dip switches and LEDs. The PCB has a protective earth frame which connects to the aluminium chassis with four mounting screws in the board's corners.

Chapter 6

Testing

The device's audio parameters were measured using a Rohde & Schwarz UPV audio analyzer, which is to be seen in Figure 6.1. The analyzer features two generator outputs and two analyzer inputs allowing for simultaneous two channel measurements.

Frequency response, THD+N (THD) and SNR measurements were performed on the stereo line inputs and outputs, mainly reflecting the contribution of the A/D and D/A converters, or possibly any errors or delays occurring in the optical conversion circuits. The same measurements were performed on the microphone preamplifier and the audio balancer separately, as both of these sections of the circuit are likely to exhibit much larger imperfections than the digital and optical conversion circuits mainly due to the Op Amp's error parameters, the higher overall number of passive components used in the analog audio path and higher susceptibility to design flaws.

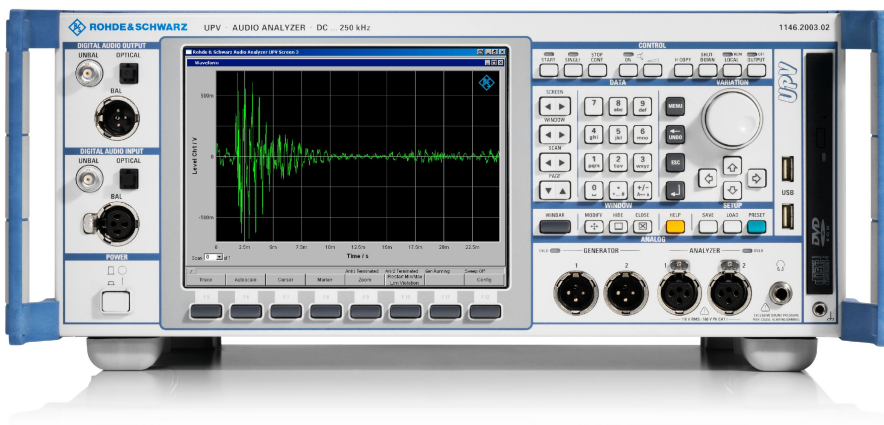


Figure 6.1: R&S UPV audio analyzer from the manufacturer's website [32]

Most of the measurements were performed (if not stated otherwise) for an audio signal level of $1 V_{RMS}$, as it is according to [4] one of the standard nominal values used for line audio in consumer electronics applications.

A signal's level can be also expressed in dBV, where $0 \text{ dBV} = 1 \text{ V}_{\text{RMS}}$. The measured frequency was in most cases 1 kHz as it is customary in audio measurements.

6.1 Line Audio

The line audio measurement results are to be examined in the following sections.

6.1.1 Frequency Response – line audio

The line audio frequency response measurement results were divided into two sections, one for the magnitude response and a another one for the phase response.

Magnitude response – line audio

The system's line audio magnitude response is to be seen in Figures 6.2, 6.3 and 6.4. Figures 6.2 and 6.3 show the magnitude's detail in the audible spectrum for an IIR and FIR interpolation and decimation filter respectively while Figure 6.4 shows the magnitude's cutoff in the higher frequency range.

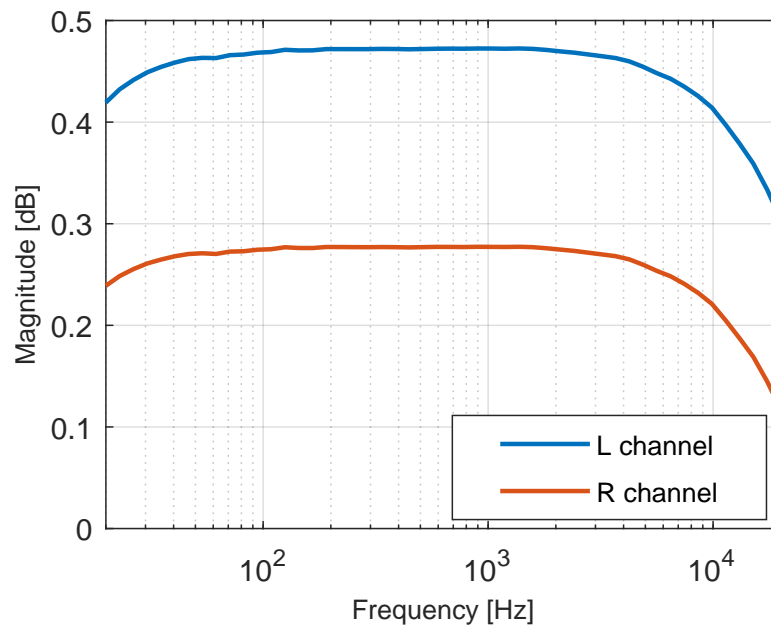


Figure 6.2: The system's measured line audio magnitude response from 20 Hz to 20 kHz with and IIR decimation and interpolation filter

Although the difference in the system's magnitude response depending on the type of filter is rather negligible, the use of an IIR decimation and interpolation filter leads to a flatter characteristics and can therefore be considered the better option in this particular matter.

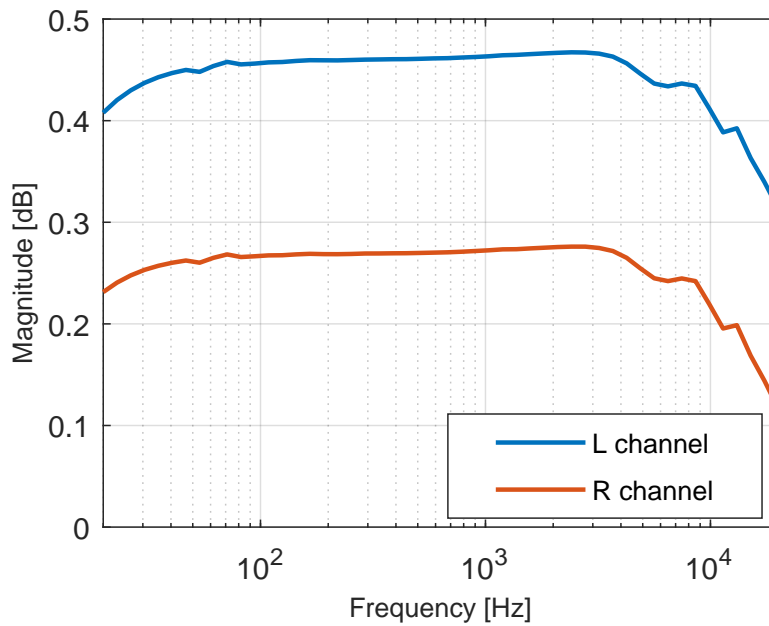


Figure 6.3: The system’s measured line audio magnitude response from 20 Hz to 20 kHz with an FIR decimation and interpolation filter

Figures 6.2 and 6.3 also show the the right channel has an approximate 0.2 dB attenuation when compared to the left channel. The reason for such attenuation has been discovered to be the right channel’s connection to the balancer circuit (described in Section 5.2.2), as after disconnecting the balancer circuit the channel’s attenuation disappears. The left channel goes directly onto the cinch connector line output. The magnitude response in the stopband is roughly the same for both an IIR and an FIR filter option, therefore only one graph (in Figure 6.4) is included.

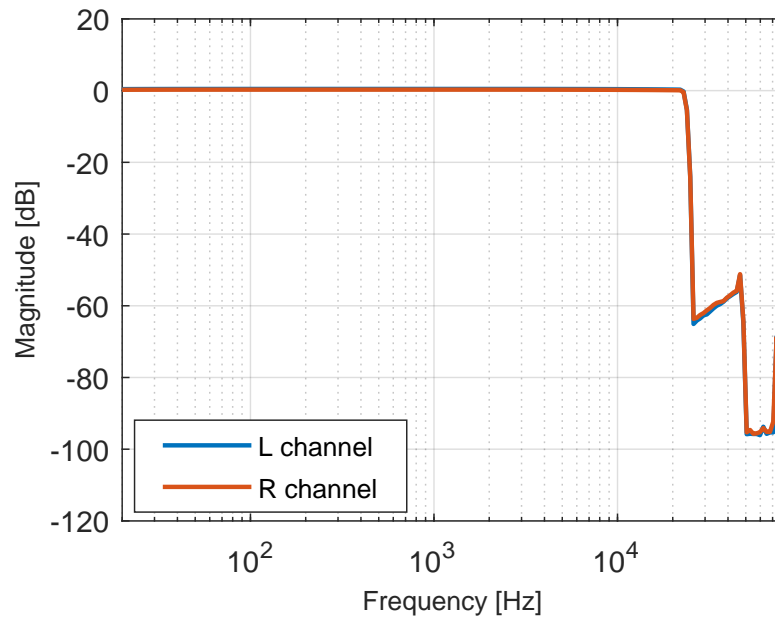


Figure 6.4: The system's measured line audio magnitude response from 20 Hz to 80 kHz

Phase response – line audio

The system's line audio phase response was measured on the left channel for both the IIR and the FIR interpolation and decimation filter. The initial measurement result is to be seen in Figure 6.5.

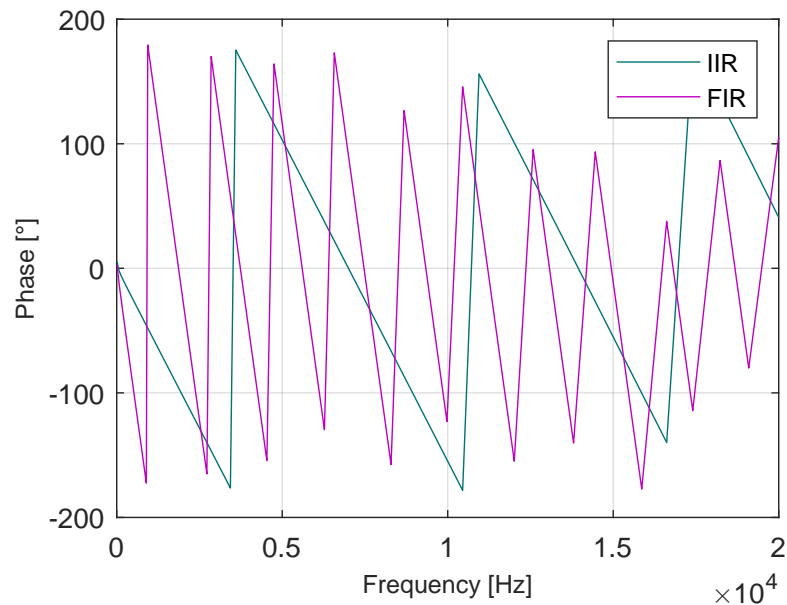


Figure 6.5: The system's measured phase response for an IIR and FIR interpolation and decimation filter

The phase response was then unwrapped in *Matlab* and the y-axis units converted into radians, as it is to be seen in Figure 6.6.

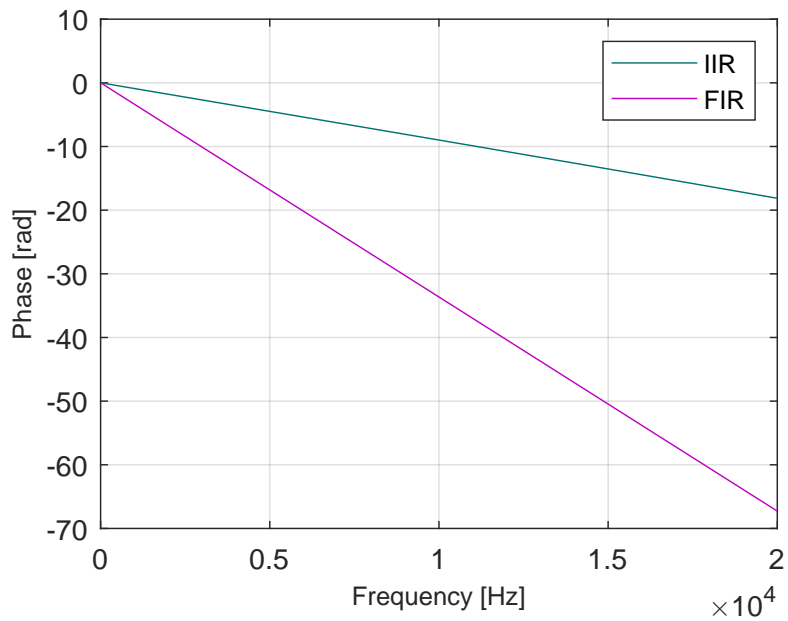


Figure 6.6: The system's unwrapped phase response for an IIR and FIR interpolation and decimation filter

By derivation of the negative unwrapped phase response in Figure 6.6 we get a group delay response, which is to be seen in Figure 6.7.

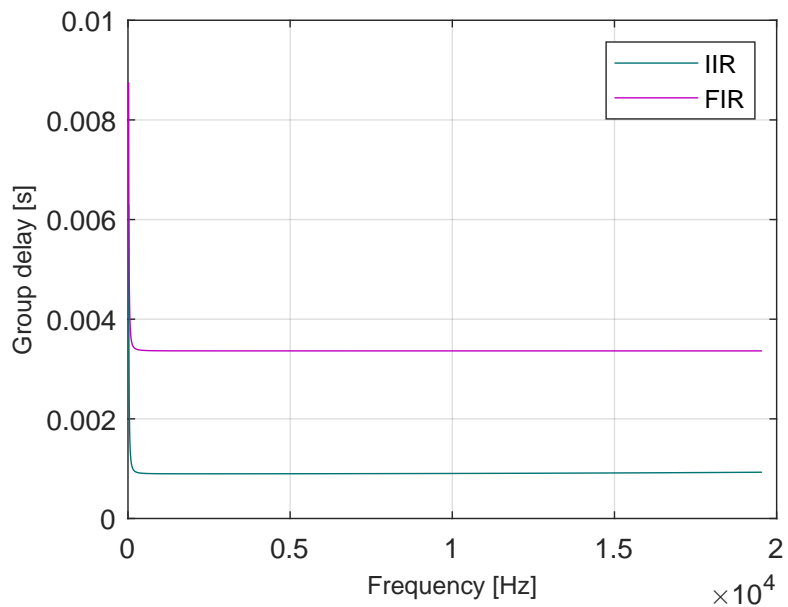


Figure 6.7: The system's group delay response for an IIR and FIR interpolation and decimation filter

Figure 6.7 shows, that by using an IIR filter we achieve a much lower latency in the transmission of the audio than in case of an FIR filter. However, Figures 6.8 and 6.9 show, that the group delay for an IIR filter is highly frequency dependent, thereby causing phase distortion, while with the FIR filter we get a constant group delay across larger part of the bandwidth.

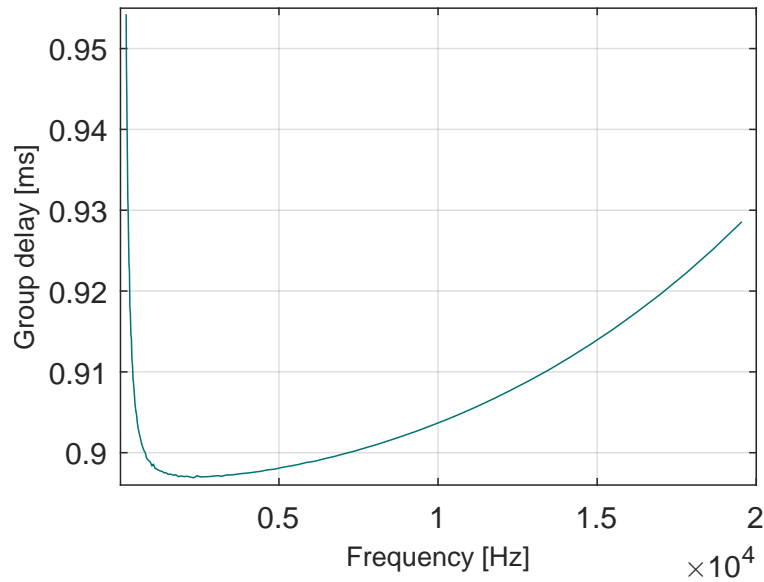


Figure 6.8: The system's group delay response for an IIR interpolation and decimation filter in detail

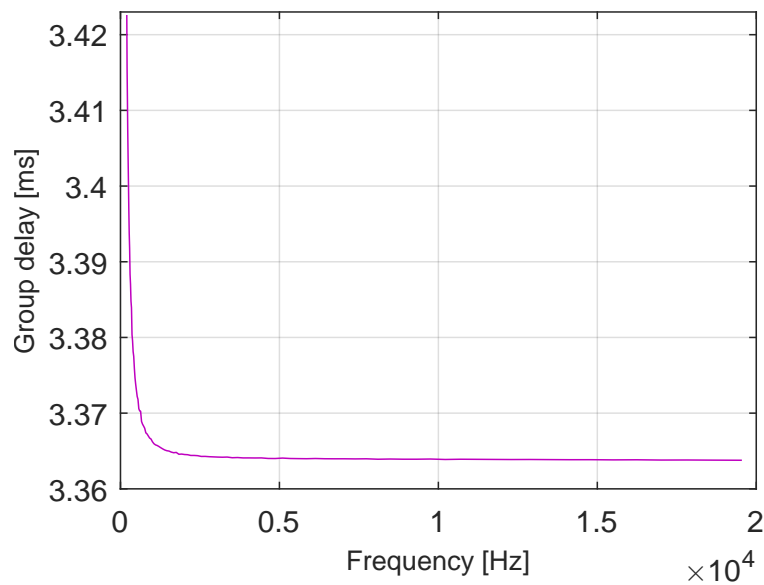


Figure 6.9: The system's group delay response for a FIR interpolation and decimation filter in detail

The substantial group delay peak at low frequencies occurring for both the IIR and FIR option is most likely caused by the converter's input analog high-pass filter. As was shown in Section 5.1.2, there are 22 μF decoupling capacitors used while the ADC's analog inputs have according to its datasheet [25] an input resistance of 20 $\text{k}\Omega$.

Since phase distortion is not a concern in our application, the IIR decimation and interpolation filters are thanks to their lower latency the preferred option.

6.1.2 THD+N – line audio

THD+N was measured for both channels for a 1 kHz sine input signal with an RMS value of 1 V. Additionally, THD+N of a direct cable connection from the UPV's generator to the UPV's analyzer was measured to demonstrate the measurement device's imperfections.

Table 6.1: Line audio's measured THD+N values

Channel	THD+N [dB]	THD+N [%]
Left	-88.5	0.0038
Right	-89.1	0.0035
<i>Direct</i>	-106.0	0.0005

The left channel and right channel output's spectra are to be seen in Figures 6.10 and 6.11 respectively. The direct connection's spectrum was also plotted in both graphs mainly to show the noise added to the audio signal in the system – the noise floor is raised by approximately 20 dB in both channels when compared to the direct connection.

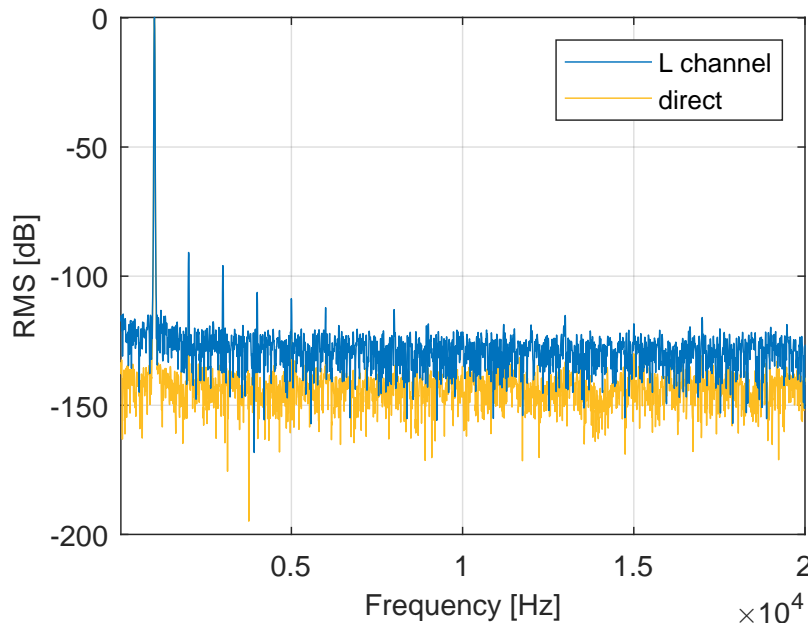


Figure 6.10: Left channel output's spectrum measured for a 1 kHz sine wave input

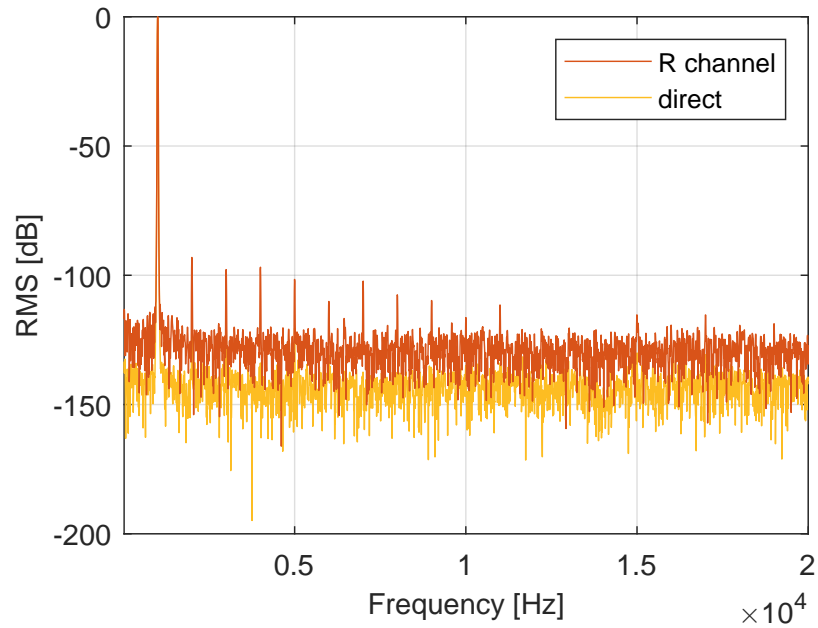


Figure 6.11: Right channel output's spectrum measured for a 1 kHz sine wave input

Although the right channel's spectrum in Figure 6.11 shows more apparent upper harmonic peaks than the left channel's spectrum in Figure 6.10, its THD+N is 0.6 dB lower. The reason for that could be higher amplitudes of the 2nd and 3rd harmonic in the left channel's spectrum, which are also the strongest of all the harmonics present in the signal as is usual for distortion in audio systems. Table 6.2 shows the amplitudes of the first five harmonic frequencies for both channels.

Table 6.2: Harmonics amplitudes in the output's spectrum for both line audio channels

Harmonics	L channel [dB]	R channel [dB]
1st	0.2	0.0
2nd	-90.8	-93.1
3rd	-95.9	-97.8
4th	-106.3	-96.8
5th	-108.7	-101.6

■ 6.1.3 SNR – line audio

The SNR was measured for both channels firstly using the UPV's integrated bandpass rectangular filter with the lower cutoff frequency of 22 Hz and the higher cutoff frequency of 20 kHz and then with an integrated A-weighting filter reflecting the equal-loudness curves.

Similarly as with THD+N measurement, The SNR of a direct connection was also measured with both filters to show the measurement device's imperfections and the noise contribution of the measured system. The measured SNR values are to be seen in Table 6.3.

Table 6.3: Line audio's SNR for different filters

Channel	SNR [dB]	
	bandpass filter	A-weighted filter
Left	97.8	100.1
Right	97.0	99.8
<i>Direct</i>	120.0	122.0

■ 6.1.4 Summary – line audio

The line audio parameters are satisfactory and stood up to the expectations. The most significant imperfection is most likely the right channel's attenuation caused by the connection to the audio balancer circuit. Frequency response measurements have shown that the IIR decimation and interpolation filter is the preferred option for our application. The measured parameters are in summary:

- 20 Hz - 20 kHz \pm 0.4 dB
- SNR \sim 100 dB (A-weighted)
- THD+N < 0.004 %

6.2 Microphone Preamplifier

The initial version of the preamplifier mounted with 100 nF C0G capacitors, 1.5 M Ω and 499 k Ω resistors at the input differential stage (to be seen in Figure 6.12) was essentially unusable due to the extreme high level of noise at the preamplifier's output, which was most likely caused by the too high feedback resistor values (see Section 1.1.1 about Johnson's noise).

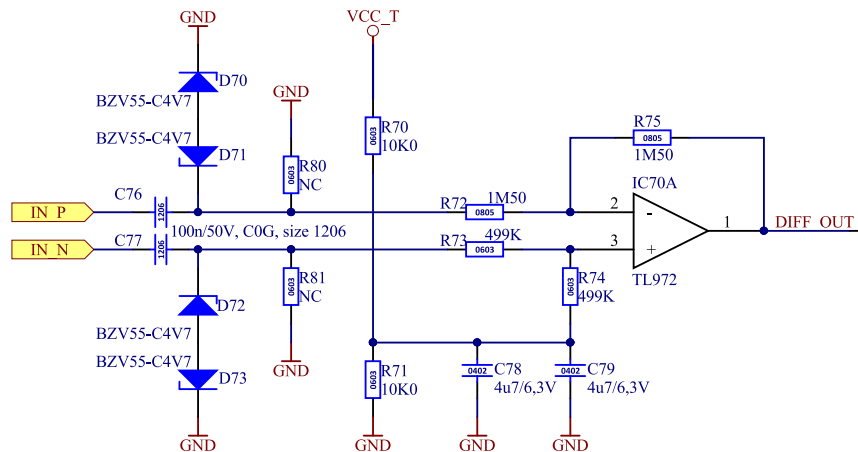


Figure 6.12: Original differential amplifier schematic

The differential stage was therefore re-mounted with higher capacity and less stable 4.7 μ F X7R capacitors so that lower value resistors could be used while preserving a flat magnitude response in the low frequency region. Figure 6.13 shows the re-mounted version with 10 k Ω and 3.3 k Ω resistors on which all the following measurements were made.

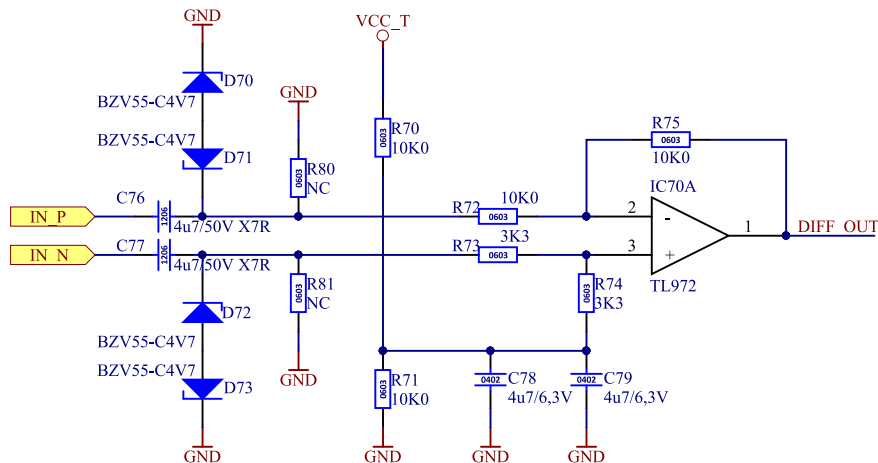


Figure 6.13: Updated differential amplifier schematic

One other variation of the differential stage with 30 k Ω and 10 k Ω resistors was also tested but showed approximately 4 dB more noise while having only tenths of decibels of improvement in its magnitude response in the low frequency range and was therefore discarded.

6.2.1 Frequency Response – preamplifier

The frequency response was measured for all four of the selectable preamplifier's gain options. Figures 6.14 and 6.15 show the frequency response for the 16 dB and the 40 dB gain option respectively.

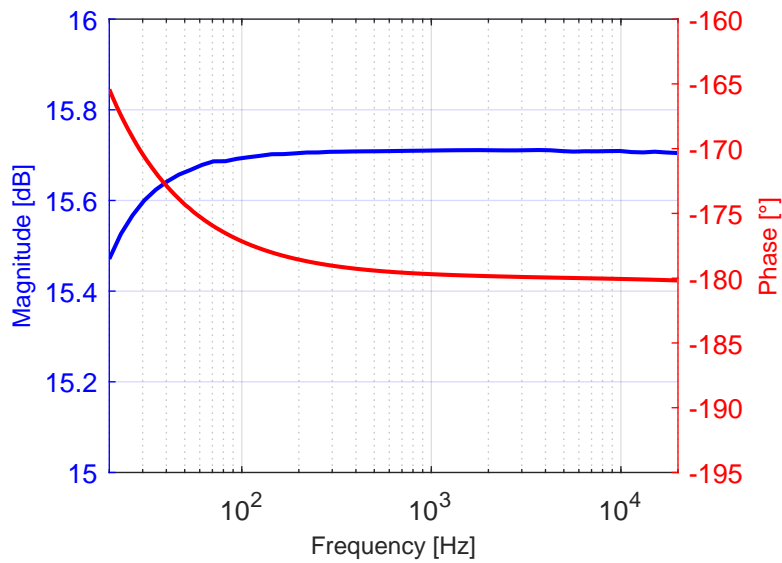


Figure 6.14: The preamplifier's measured frequency response for a gain of 16 dB

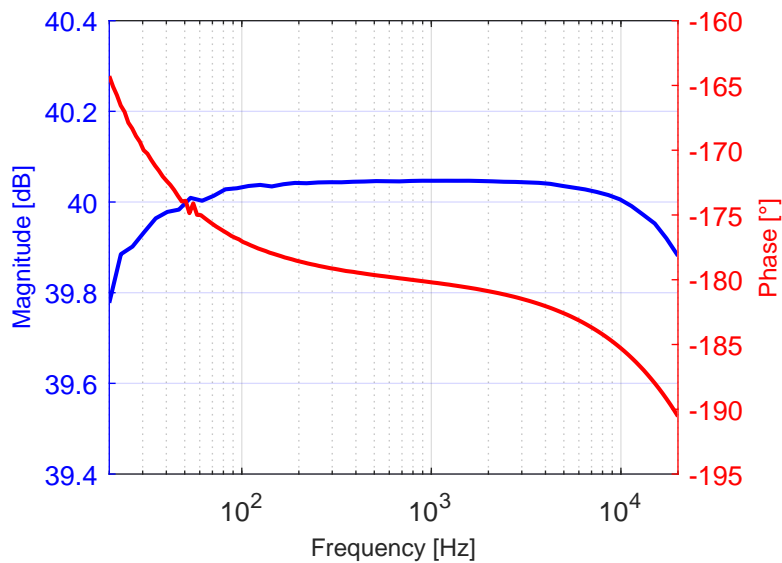


Figure 6.15: The preamplifier's measured frequency response for a gain of 40 dB

Figure 6.15 shows a slight presence of a power distribution network interference at 50 Hz. The overall ripple of the magnitude response in the low frequency region is higher for the 40 dB option, which is likely caused by the higher level of noise (to be further examined in Section 6.2.3). The preamplifier inverts the signal's phase which could be prevented by either switching the positive and negative input at the preamplifier's first differential stage or using an inverting wiring of the preamplifier's second stage instead of a non-inverting one.

6.2.2 THD+N – preamplifier

As the noise levels were unusually high for this circuit, THD was also measured as THD+N wasn't indicative of the amplifier's actual distortion. Table 6.4 shows the measurement results for different gains. The input level was tweaked for each gain setting to set the proper output level of $1 V_{RMS}$.

Table 6.4: The preamplifier's THD+N and THD values for different gains

Gain	THD+N [dB]	THD [dB]	THD [%]
16 dB	-91.9	-99.0	0.0011
20 dB	-87.4	-97.5	0.0013
40 dB	-68.4	-78.6	0.0117
50 dB	-52.3	-58.2	0.1230
bypass	-94.8	-95.8	0.0018

6.2.3 SNR – preamplifier

SNR was measured for all four available preamplifier's gain settings as well as for the preamp bypass setting which takes the output directly from the differential amplifier. The measured SNR values are to be seen in Table 6.5. The input level was tweaked for each gain setting same as in case of THD measurements.

Table 6.5: Preamplifier's SNR values for different gains and two different filters

Gain	SNR [dB]	
	bandpass filter	A-weighted filter
16 dB	91.9	95.1
20 dB	86.9	90.1
40 dB	67.8	70.9
50 dB	54.6	57.7
bypass	102.8	106.4

As we can see in Table 6.5, SNR values for the bandpass filter are almost exactly the inverse values of THD+N from Table 6.4 which by itself only demonstrates the inadequately high level of noise in the circuit. Furthermore, we can see that by applying the A-weighted filter, we decrease SNR by approx. 3 to 4 dB when compared to the bandpass filter. The explanation for that

could be the frequency distribution of noise and the dominance of flicker noise (see Section 1.1.3 about flicker noise), which has the highest effect in the lower frequency region, where the human ear isn't as sensitive. Figure 6.16 shows the noise's FFT in the low frequency region for a 20 dB gain setting.

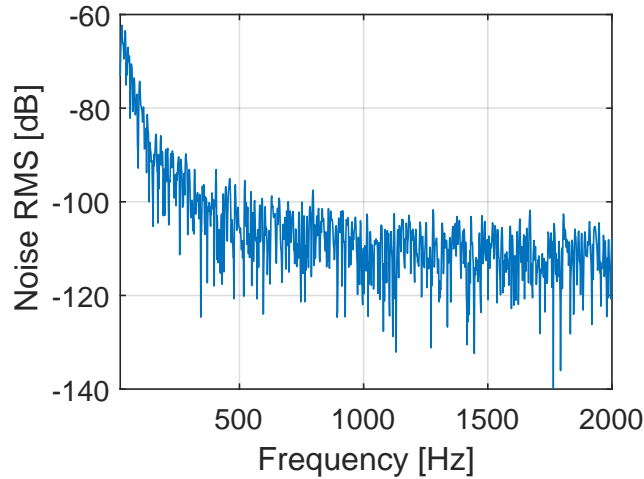


Figure 6.16: FFT of the preamp's output's noise for a gain of 20 dB

Given that the SNR value is directly proportional to the amplifier's gain, we can obtain the equivalent input noise value (EIN), by calculating the noise RMS value and dividing it by the gain. The value should be approximately the same for all the measured gains. By modifying Equation 1.2 we can obtain the following Equation to calculate the EIN of the circuit

$$\text{EIN} = V_{\text{out}} \times 10^{-\frac{\text{SNR}_{\text{dB}} + \text{Gain}_{\text{dB}}}{20}}, \quad (6.1)$$

where V_{out} is the output RMS voltage, SNR_{dB} is the signal-to-noise ratio in decibels and Gain_{dB} is the amplifier's gain. The obtained EIN value when averaging the different gain settings for the A-weighted filter is approximately -110 dBV.

■ 6.2.4 CMRR

The preamplifier's CMRR in relation to frequency is to be seen in Figure 6.17. The values were measured for a 1 V_{RMS} common mode input with a frequency sweep. The y-axis was plotted in dBV and subsequently inverted to obtain the CMRR values.

The differential stage is mounted with 1% tolerance resistors which most likely has a huge negative impact on CMRR, as the resistors in the differential stage have to be according to [4] matched as closely as possible to reach the best possible suppression of common mode signal – e.g. an electromagnetic interference. In the future, ideally 0.1% tolerance resistors are to be mounted. The author also states that it is typical that CMRR will eventually start decreasing with frequency and may also deteriorate at low frequencies, which is our case.

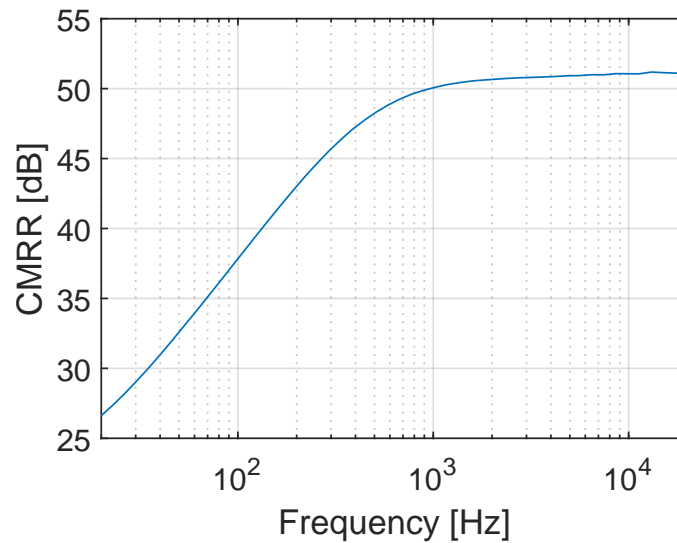


Figure 6.17: Measured CMRR of the differential stage in relation to frequency

Simulations have shown, that raising the resistor values in the differential stage leads to better CMRR, although it also naturally increases noise. Currently, the CMRR value at 1 kHz is around 50 dB which is an underwhelming result even worse than the differential amplifier integrated in the PCM1861 A/D converter, which features differential inputs with a typical CMRR of 56 dB as listed in the part's datasheet [25].

In [4] the author marks the use of our current combination of resistors in the differential stage (where two of the resistor values are one-third of the other two) as undesirable, as although it matches the input impedances for a differential signal,

"... it degrades the noise performance markedly and makes the common-mode impedances to ground unequal." (Douglas [4], 2015, p. 498).

The author also describes a so-called *Superbal* circuit, which is to be seen in Figure 6.18, and which has matching input impedances for both common mode and differential input and thereby provides high CMRR. Its only disadvantage is a 6 dB attenuation to the balanced input.

■ 6.2.5 Summary – preamplifier

The preamplifier's performance is underwhelming especially due to its high noise levels. Its distortion levels would likely be improved by increasing the power supply voltage to e.g. 5 V and its CMRR should be somewhat improved by remounting the resistors with lower tolerance ones.

Although the preamplifier's phase shift hasn't been considered to be an inconvenience, it could be prevented by either switching the first stage's positive and negative input or simply using an inverting second stage instead of a non-inverting one.

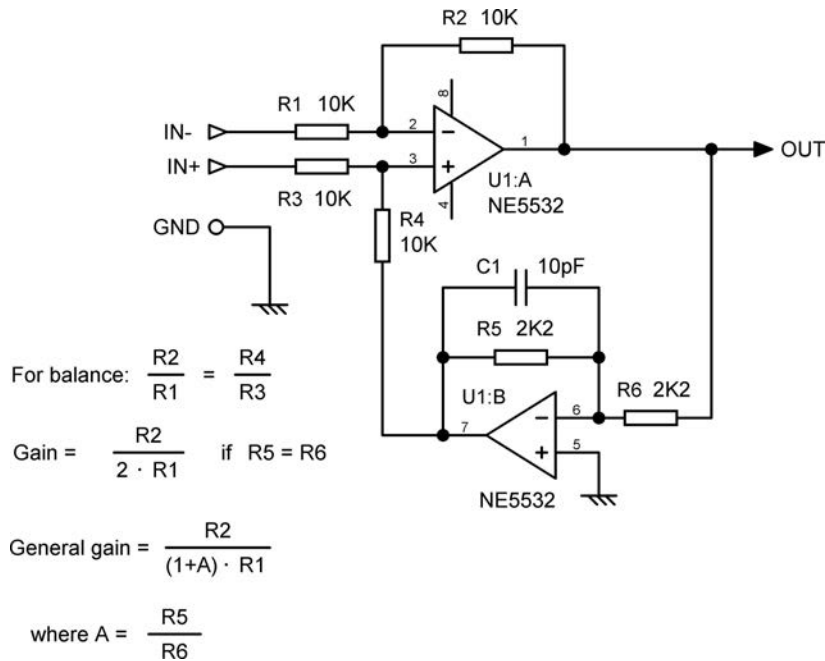


Figure 6.18: A *Superbal* input amplifier from [4], p. 509

In [4] the author claims, that to fulfill the low-noise requirements for a microphone preamplifier, it should include hybrid input stages combining discrete transistors and Op Amps, as discrete transistors give much lower noise while Op Amps provide open-loop gain and load-driving capability. Furthermore, it is stated that a microphone preamplifier should ideally provide up to 70 dB of gain.

The designed preamplifier is somewhat usable only up to 40 dB of gain where its SNR reaches a value of around 70 dB. Such gain is by all means not sufficient for most dynamic microphones which usually require a gain of more than 60 dB to reach the consumer line level of 1 V_{RMS} due to their low sensitivity. Some condenser microphones sensitivity can go up to around -30 dB, in which case the preamplifier's capabilities could be sufficient, although the four discrete gain settings most likely wouldn't allow to set up the preamplifier for the best possible performance and the SNR would still remain quite high.

To improve the preamplifier's noise performance, the amplification itself could be performed in the first differential stage instead of the subsequent non-inverting stage, as in [8] it is stated that after an amplification in the input stage the subsequent stages have minimal contribution of noise. The differential stage though doesn't provide very convenient gain setting possibilities, as at least two individual resistor values have to be changed to effectively change the stage's gain while both of these values should remain as close to each other as possible to retain good CMRR.

Considering all the above, the entire preamplifier is likely going to be fully redesigned, possibly with a discrete transistor input stage such as the one that can be seen in Figure 6.19. The circuit in Figure 6.19 though it produces very low noise is quite susceptible to distortion and requires additional Op Amps to implement a balanced feedback to lower its distortion. With all those extra necessary components the overall production price of the device will considerably increase.

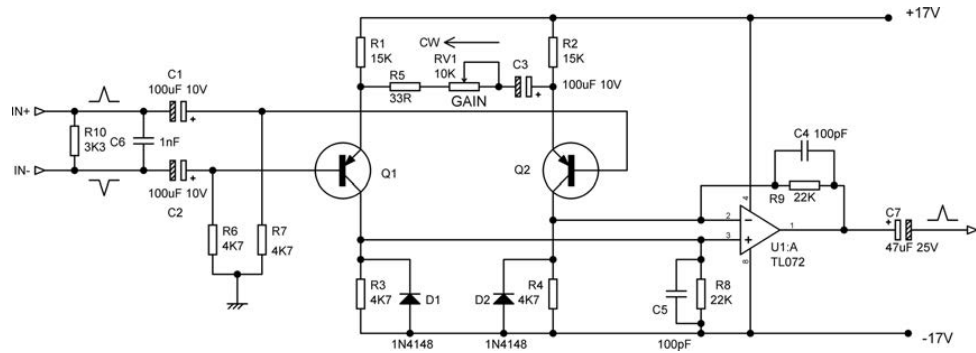


Figure 6.19: Simple hybrid microphone preamplifier from [4] p. 501

6.3 Audio Balancer

The audio balancer's measurement results are to be examined in the following sections. The UPV audio analyzer was set to process a balanced input signal for all the listed measurements.

6.3.1 Frequency Response – balancer

Figure 6.20 shows the measured frequency response, which almost perfectly matches the LTSpice simulations from Section 5.2.2 covering the circuit's schematic design. The slight differences in the characteristics is likely caused by the part's value tolerances.

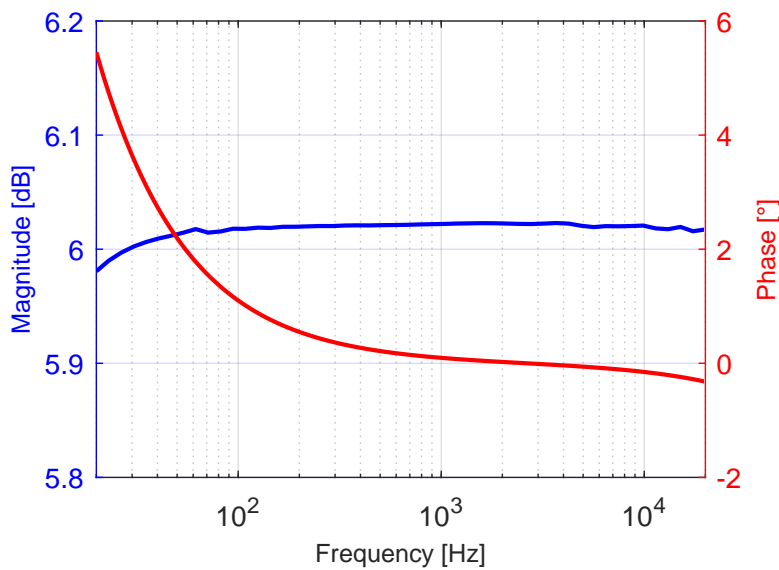


Figure 6.20: The balancer's measured frequency response

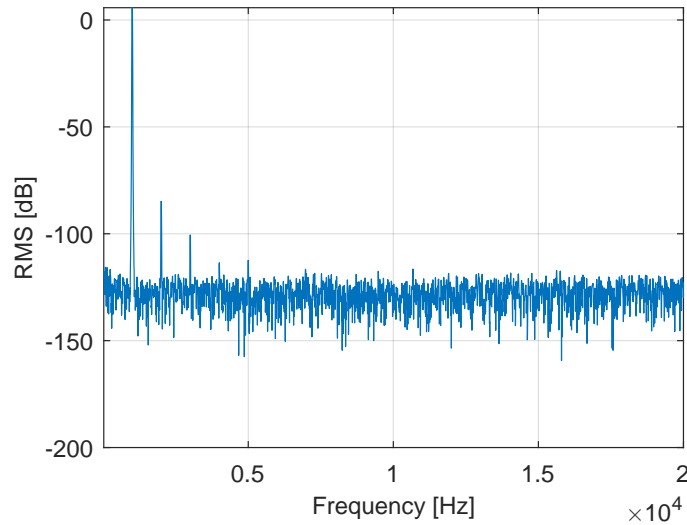
6.3.2 THD+N – balancer

The balancer's THD+N was measured for multiple input levels, as can be seen in Table 6.6. Since the Op Amp's output signal amplitude is obviously limited by half of the power supply voltage, which in our case is 1.65 V, we can see that the circuit's distortion starts increasing significantly as the input peak voltage approaches that value. The breakthrough occurs at the input peak of 1.4 V, where the large growth of distortion starts, and where the signal is, unfortunately, only at approx. 85 % of the circuit's full scale voltage.

Table 6.6: Balancer's THD+N values for different input levels

Input RMS [V]	Input peak [V]	THD+N [dB]	THD+N [%]
0.1	0.14	-86.7	0.005
0.2	0.28	-90.2	0.003
0.3	0.42	-93.2	0.002
0.4	0.57	-91.9	0.003
0.5	0.71	-90.2	0.003
0.6	0.85	-88.0	0.004
0.7	0.99	-85.6	0.005
0.8	1.13	-82.0	0.008
0.9	1.27	-73.9	0.020
1.0	1.41	-59.3	0.108
1.1	1.56	-44.8	0.575
1.2	1.70	-29.3	3.428

Figures 6.21 and 6.22 show the output's spectrum for a 0.5 V and 1 V RMS input respectively. The significant difference between the two spectra which is obvious at first glance as the number and height of the peaks in the second spectrum far outreach the first spectrum is the cause for more than a 30 dB difference in THD+N.

**Figure 6.21:** FFT of the balancer's output measured for a 0.5 V_{RMS} sine wave 1 kHz input

Considering that the line level of an audio signal is according to [4] typically around 1 V_{RMS} (depending on the type of audio device), THD+N of 0.108 % at such input level is a rather underwhelming result. As can be seen in the Op Amp's datasheet [27], distortion is heavily dependent on the load impedance used. Unfortunately the UPV analyzer only allows for the use of either 300 Ω, 600 Ω or 200 kΩ measuring impedance, whereas the first two impedances are lower than what the Op Amp can drive.

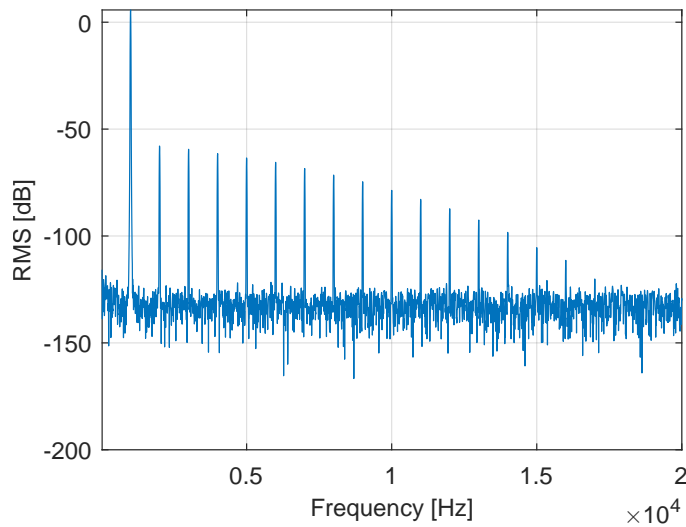


Figure 6.22: FFT of the balancer's output measured for a $1 V_{\text{RMS}}$ sine wave 1 kHz input

All the measurements were therefore performed with a $200 \text{ k}\Omega$ load, which is a relatively high value and the distortion results would probably come out even worse using a lower measuring impedance.

If we look at Figure 6.23 from the Op Amp's datasheet [27], we see that for a $2 \text{ k}\Omega$ load and a 2.7 V power supply voltage the 0.1% THD+N value is reached for a peak-to-peak voltage of around 1.65 V which is only around 61% of the supply voltage for which the measurement was performed.

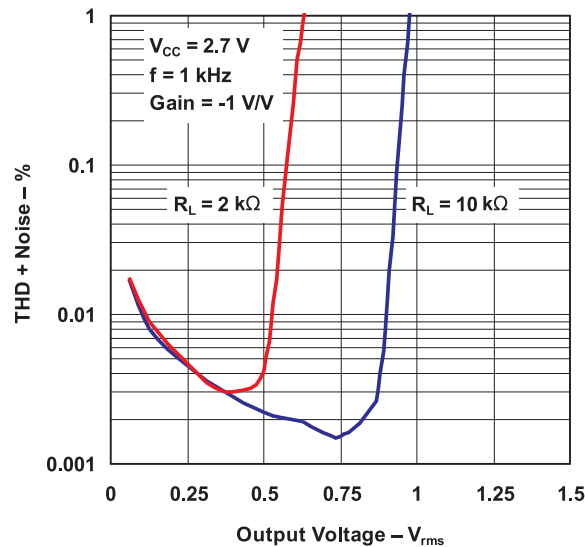


Figure 6.23: TL972 dependence of THD+N on the output's RMS voltage for a 2.7 V power supply voltage from the part's datasheet [27]

Figure 6.24 shows THD+N for a 5 V power supply voltage and the results are clearly much better than in the previous case. THD+N of 0.1% is reached at around 4.84 V peak-to-peak voltage which is almost 97 % of the supply voltage for the same load impedance of 2 k Ω .

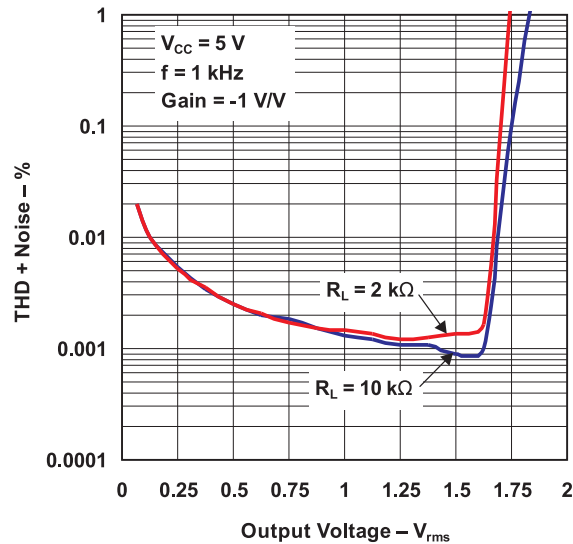


Figure 6.24: TL972 dependence of THD+N on the output's RMS voltage for a 5 V power supply voltage from the part's datasheet [27]

The information above leads us to a possible solution to decrease the circuit's THD+N at higher input levels, which would be to increase the Op Amps' power supply voltage to achieve a larger headroom. Such modification would require additional circuitry to then step-down the power supply voltage to the 3.3 V value required by the D/A converter which would further raise the cost of the product.

6.3.3 SNR – balancer

Given that the balancer's magnitude frequency response comes close to being perfectly flat across the entire audible spectrum, the frequency on which SNR was measured had only a negligible impact on the measured values. Table 6.7 shows the SNR values for a 1 kHz sine wave input.

Table 6.7: Balancer's SNR values for different input levels and two different filters

Input RMS [V]	SNR [dB]	
	bandpass filter	A-weighted filter
1.00	107.1	109.2
0.50	101.0	103.3
0.25	95.0	97.3

We can see that by reducing the input level by half (i.e. by 6 dB), SNR as expected decreases by 6 dB, as the noise floor is constant and independent of the input signal. By modifying Equation 1.2 we can obtain the following Equation to calculate the noise RMS voltage

$$V_n = \frac{V_{in}}{10^{\frac{SNR_{dB}}{20}}}, \quad (6.2)$$

where V_n is the noise RMS voltage, V_{in} is the input RMS voltage and SNR_{dB} is the signal-to-noise ratio in decibels. The calculated noise RMS values are to be seen in Table 6.8.

Table 6.8: The balancer's noise RMS values

filter	Noise RMS [μ V]
bandpass	4.42
A-weighted	3.47

6.3.4 Summary – balancer

The circuit's distortion levels are unfortunately underwhelming. Although there are dedicated balanced audio line drivers integrated circuits such as DRV134UA from Texas Instruments or 1646 from THAT with much lower distortion, they all require a symmetrical power supply of around ± 5 V and are much more expensive than the current solution with the TL972 operational amplifiers.

Raising the balancer's power supply voltage to e.g. 5 V as was examined in Section 6.3.2 is one of the possible solutions to the high distortion levels. Otherwise the circuit's noise and frequency response stood up to the expectations. It is also important to remind that the total balanced output level is actually twice the input level and for an input level of $0.5 V_{RMS}$ where the output is at the standard line level of $1 V_{RMS}$ the THD+N is only 0.003 % which is a very positive result.

The measured parameters for a 0 dBV input signal level and an A-weighted filter are:

- 20 Hz - 20 kHz ± 0.1 dB
- SNR ~ 109 dB
- THD+N ~ 0.1 %¹

¹0.003 % for a 0 dBV output signal level

6.4 Miscellaneous

This section is meant for the remaining results of tests and measurements which weren't covered in the previous sections.

All three power supply blocks work properly and output the desired voltage. Noise RMS voltage in the audible frequencies was measured on the analog and digital 3.3 V power supply and the results were 850 μV RMS for the analog power supply using the LT3012B linear regulator and 165 μV RMS for the digital power supply using the TPS54160 buck converter.

The LT3012B regulator is unfortunately also used to produce the phantom power polarization voltage, and its performance in this case is due to the high level of added noise rather unsatisfactory. The use of condenser microphones in combination with the noisy preamplifier is not desirable on the current version of the device, as both the preamplifier and the phantom power would first have to be redesigned to bring the noise levels to a level that is acceptable for high-end audio applications.

Parts of the layout and routing on the PCB were executed inappropriately, namely the audio signal routes, as the board is susceptible to EMI from digital communication of surrounding electronic devices, and unwanted interference is sometimes to be heard in the audio. Although the issue would likely be solved by placing the PCBs in one of the company's aluminium chassis which provides shielding, the PCBs are currently exposed as the aluminium chassis is yet to be cut for the next version of the device which is likely to have an updated component placement.



Conclusion

This thesis was devoted to audio signal processing for optical transmission. In the Theoretical Part of this thesis, the principles of analog signal processing including noise, distortion and parameters of Op Amps were covered, followed by the process of digitization of audio signals as well as digital filters and serial protocols for digital audio transmission. Finally, the basics of optical communication were outlined.

The main focus of the Practical Part was then the design and testing of an audio processing system for optical transmission. The designed device features balanced and stereo audio inputs and outputs and a microphone preamplifier supporting dynamic, electret and condenser microphones.

The system utilizes the PCM1861 A/D converter and the PCM5102A D/A converter, both of which use the I²S serial protocol for the digital audio transmission. The tests and measurements proved the stereo audio transmission to meet the expectations, as its SNR was measured to be around 100 dB and its THD+N below 0.004 %. The balanced audio path, however, due the high levels of noise, low CMRR and unsatisfactory distortion is to be fully redesigned for the next version.

It was decided that a microphone preamplifier of sufficient quality would exceed the required production costs and isn't a fundamental feature for the company's potential customers. Because of that, the next version of the device is to feature only a balanced input, probably implemented with the *Superbal* circuit from Figure 6.18, without any gain capabilities and thus without any support for microphones.

Furthermore, an inverter is to be used on the analog 3.3 V power supply to allow a symmetrical powering of the Op Amps, thereby increasing headroom and lowering distortion as well as eliminating the need for the many passive components necessary to properly bias the Op Amps, thanks to which it is expected to be a more cost-effective solution. The symmetrical power supply will also improve switching capabilities on the receiver's side, as it then will be possible to use the TS3A24157 electronic switches to switch the DAC ground centered outputs.

The effects of noise, distortion and EMI were unfortunately underestimated in the design process of both the analog front-end and the PCB. The overall efforts of this thesis can, however, be considered a success, as a functioning prototype of an audio transmission system was produced and set the groundwork for future versions with improved parameters.



Bibliography

- [1] SOLANKI, Khusbu. *Fibre Optics vs Copper Cabling - Understanding the Difference* [online]. Datatronix, 5 [quot. 2023-03-20]. Available from: https://datatronix.com/downloads/whitepapers/DT_Fibre_Optics_vs_Copper_Cabling_Understanding_the_Difference_White_Paper_Rev.1.0.pdf
- [2] NOVOTNÝ, Karel, 2007. *Optická komunikační technika*. Prague: CTU. ISBN 978-80-01-03920-5
- [3] *AN-806 Data Transmission Lines and Their Characteristics* [online]. Texas Instruments, 2004, 10 [quot. 2023-03-20]. Available from: <https://www.ti.com/lit/an/snla026a/snla026a.pdf>
- [4] SELF, Douglas. *Small Signal Audio Design*. 2nd edition. Burlington, MA: Focal Press, 2015. ISBN 9780415709736
- [5] PUTHUSSERYPADY, Sadasivan, 2021. *Applied Signal Processing*. Hanover, MA: Publishers. ISBN 978-1-68083-978-4
- [6] HAMDY, Nadder. *Applied Signal Processing: Concepts, Circuits, and Systems*. Boca Raton, Florida: CRC Press, 2008. ISBN 978-1-4200-6702-6
- [7] STEPHAN, Karl. *Analog and Mixed-Signal Electronics*. Hoboken, New Jersey: Wiley, 2015. ISBN 978-1-118-78266-8
- [8] VEDRAL, Josef & Jakub SVATOŠ. *Analog Signal Processing and Digitalization in Measurement*. Prague: CTU, 2020. ISBN 978-80-01-06717-8
- [9] KIELY, Robert. Understanding and Eliminating 1/f Noise. *Analog Dialogue* [online]. May 2017, 55(05), 4. Available from: <https://www.analog.com/media/en/analog-dialogue/volume-51/number-2/articles/understanding-and-eliminating-1-f-noise.pdf>
- [10] *Op Amp Distortion: HD, THD, THD + N, IMD, SFDR, MTPR* [online]. Analog Devices, 2009, 8 [quot. 2022-11-13]. Available from: <https://www.analog.com/media/en/training-seminars/tutorials/MT-053.pdf>

- [11] PASS, Nelson. Audio distortion and feedback. *Technical Articles* [online]. Pass Laboratories, 2008 [quot. 2022-12-01]. Available from: https://www.passlabs.com/technical_article/audio-distortion-and-feedback/
- [12] HAASZ, Vladimír a kolektiv. *Elektrická měření: Přístroje a metody*. 3rd edition. Prague: CTU, 2018. ISBN 978-80-01-06412-2
- [13] HOSPODKA, Jiří. Reálné vlastnosti operačního zesilovače. *Electronic Circuits 2* [online]. Prague, 61 [cit. 2022-11-30]. Available from: https://hippo.feld.cvut.cz/vyuka/soubory/oz_re.pdf
- [14] EARGLE, John, 2005. *The Microphone book*. 2nd edition. Oxford: Focal Press. ISBN 0240519612
- [15] NOYES, Tyler, Alex DAVIS a Aldwin DELCOUR. *Phantom Power with Operational Amplifiers* [online]. Texas Instruments Incorporated, November 2018, 4 [quot. 2022-10-30]. Available from: <https://www.ti.com/lit/pdf/sboa320>
- [16] LEWIS, Jerad. *Common Inter-IC Digital Interfaces for Audio Data Transfer* [online]. 2020, 3 [quot. 2022-10-16]. Available from: <https://www.analog.com/media/en/technical-documentation/technical-articles/MS-2275.pdf>
- [17] MIAO, George J. *Signal Processing in Digital Communications*. Artech House, 2006. ISBN 9781580536677
- [18] 13.9: Delta-Sigma ($\Delta\Sigma$) ADC, 2007. In: R. KUPHALDT, Tony. *Lessons In Electric Circuits, Volume IV – Digital* [online], Available from: <https://www.allaboutcircuits.com/assets/pdf/digital.pdf>.
- [19] BAKER, Bonnie. How delta-sigma ADCs work, Part 1 *Analog Design Journal* [online]. Texas Instruments Incorporated, 2011, 11(3), 6. Available from: <https://www.ti.com/lit/an/slyt423a/slyt423a.pdf>
- [20] *Sigma-Delta ADCs and DACs Application Note (AN-283)* [online]. Analog Devices, 16 [quot. 2023-04-19]. Available from: <https://www.analog.com/media/en/technical-documentation/application-notes/292524291525717245054923680458171an283.pdf>

- [21] CHEUNG, Hugo & Sreeja RAJ. Implementation of 12-bit delta-sigma DAC with MSC12xx controller. *Analog Applications Journal* [online]. Texas Instruments Incorporated, 5(1), 7 [quot. 2023-04-19]. Available from: <https://www.ti.com/lit/an/slyt076/slyt076.pdf>
- [22] *Interfacing PDM digital microphones using STM32 MCUs and MPUs: AN5027* [online]. STMicroelectronics, 2019, 66 [quot. 2022-13-11]. Available from: https://www.st.com/resource/en/application_note/dm00380469-interfacing-pdm-digital-microphones-using-stm32-mcus-and-mpu-stmicroelectronics.pdf
- [23] AGRAWAL, Govind P., 2010. *Fiber-Optic Communication Systems*. Fourth edition. Hoboken, New Jersey: Wiley. ISBN 978-0-470-50511-3
- [24] KAYE, Zak. Selecting capacitors to minimize distortion in audio applications. *Analog Design Journal* [online]. Texas Instruments Incorporated, 2020, 20(3), 6. Available from: <https://www.ti.com/lit/an/slyt796/slyt796.pdf>
- [25] Texas Instruments, *PCM1861* datasheet [online]. 2014, p. 144 [quot. 2023-01-24]. Available from: <https://www.ti.com/lit/ds/symlink/pcm1861.pdf>
- [26] Texas Instruments, *PCM5102A* datasheet [online]. 2012, p. 45 [quot. 2023-01-24]. Available from: <https://www.ti.com/lit/ds/symlink/pcm5102a.pdf>
- [27] Texas Instruments, *TL972* datasheet [online]. 2006, p. 35 [quot. 2022-10-06]. Available from: <https://www.ti.com/lit/ds/symlink/tl972.pdf>
- [28] Neutrik, *NCJ6FA-H* datasheet [online]. p. 2 [quot. 2022-10-06]. Available from: <https://cz.mouser.com/datasheet/2/289/ncj6fah-2-1854048.pdf>
- [29] Texas Instruments, *TS3A24157* datasheet [online]. 2007, p. 30 [quot. 2023-04-06]. Available from: <https://www.ti.com/lit/ds/symlink/ts3a24157.pdf>
- [30] Texas Instruments, *TPS54160* datasheet [online]. 2012, p. 58 [quot. 2023-01-22]. Available from: <https://www.ti.com/lit/ds/symlink/tps54160.pdf>
- [31] Analog Devices, *LT3012B* datasheet [online]. 2006, p. 16 [quot. 2023-01-29]. Available from: <https://www.analog.com/media/en/technical-documentation/data-sheets/3012bf.pdf>
- [32] R&S UPV audio analyzer: *Compact instrument for all audio measurements* [online]. [quot. 2023-05-06]. Available from: https://www.rohde-schwarz.com/us/products/test-and-measurement/audio-analyzers/rs-upv-audio-analyzer_63493-7558.html



Appendices

Appendix A

List of Abbreviations

Abbreviation	Meaning
A/D	Analog to Digital
ADC	Analog to Digital Converter
BCD	Binary Coded Decimal
BER	Bit Error Rate
CMRR	Common Mode Rejection Ratio
D/A	Digital to Analog
DAC	Digital to Analog Converter
DSP	Digital Signal Processing
ECAD	Electronic Computer-Aided Design
EIN	Equivalent Input Noise
EMI	Electromagnetic Interference
FFT	Fast Fourier Transform
FIR	Finite Impulse Response
IC	Integrated Circuit
IIR	Infinite Impulse Response
LJ	Left-Justified
LSB	Least Significant Bit
MLCC	Multilayer Ceramic Capacitor
MSB	Most Significant Bit
Op Amp	Operational Amplifier
PCB	Printed Circuit Board
PCM	Pulse-Code Modulation
PDM	Pulse-Density Modulation
PGA	Programmable Gain Amplifier
PLC	Programmable Logic Controller
RJ	Right-Justified
SE	Single-Ended
SFP	Small Form-factor Pluggable
SNR	Signal to Noise Ratio
SPDT	Single Pole Double Throw
TDM	Time Division Multiplex
THD	Total Harmonic Distortion
THD+N	Total Harmonic Distortion Plus Noise